MATERIALS CENTRAL TECHNICAL LIBRARY
OFFICIAL FILE COPY

WADD-TR-60-869
Part II

AD-278 746

EFFECT OF STATE OF STRESS ON THE FAILURE OF METALS AT VARIOUS TEMPERATURES

TECHNICAL DOCUMENTARY REPORT NO. WADD 60-869, Part II

June 1962

Directorate of Materials and Processes
Aeronautical Systems Division
Air Force Systems Command
Wright-Patterson Air Force Base, Ohio

Project No. 7353, Task No. 735301

(Prepared under Contract No. AF 33(616)-6041 by The University of Michigan, Ann Arbor, Michigan; R. M. Haythornthwaite and D. R. Jenkins, authors.)

NOTICES

When Government drawings, specifications, or other data are used for any purpose other than in connection with a definitely related Government procurement operation, the United States Government thereby incurs no responsibility nor any obligation whatsoever; and the fact that the Government may have formulated, furnished, or in any way supplied the said drawings, specifications, or other data, is not to be regarded by implication or otherwise as in any manner licensing the holder or any other person or corporation, or conveying any rights or permission to manufacture, use, or sell any patented invention that may in any way be related thereto.

Qualified requesters may obtain copies of this report from the Armed Services Technical Information Agency, (ASTIA), Arlington Hall Station, Arlington 12, Virginia.

This report has been released to the Office of Technical Services, U.S. Department of Commerce, Washington 25, D.C., in stock quantities for sale to the general public.

Copies of this report should not be returned to the Aeronautical Systems Division unless return is required by security considerations, contractual obligations, or notice on a specific document.

400 - August 1962 - 42-1843 ‡ 1844

FOREWORD

This report was prepared by The University of Michigan under USAF Contract No. AF 33(616)-6041. The contract was initiated under Project No. 7021, "Solid State Research and Properties of Matter," Task No. 73653, "Mechanisms of Flow and Fracture of Metallic and Non-Metallic Crystalline Substances. The contract is now under Project No. 7353, "Characterization of Solid Phase and Interphase Phenomena in Crystalline Substances," Task No. 735301, "Mechanical Metallurgy."

The work was under the direction of the Directorate of Materials and Processes, Deputy Commander/Technology, Aeronautical Systems Division, with Dr. J. A. Herzog acting as project engineer.

This report covers work conducted from 1 January 1961 to 31 January 1962.

ABSTRACT

Experimental observations of initial yielding, strain hardening, and fracture of Zamak-3 tubes for various states of combined stress are presented. Testing temperatures of 32°F and 78°F were employed. These observations are compared with predictions of Mises, Tresca, and maximum reduced stress theories of initial yielding and with isotropic and kinematic theories of strain-hardening. Fracture data are compared with the Griffith theory of rupture for brittle materials.

It is concluded that Zamak-3 behaves as an essentially isotropic material in which yielding is independent of mean stress. Multiple loading path test results agree rather well with the predictions of kinematic hardening theory in conjunction with the Tresca yield criterion. Fracture results conform to a maximum normal stress theory which coincides with the Griffith theory for the stress combinations investigated.

45 21 fy

PUBLICATION REVIEW

This technical documentary report has been reviewed and is approved.

B. K. Morse

B. K. MORSE
Acting Chief,
Advanced Metallurgical Studies Branch
Metals & Ceramics Laboratory
Directorate of Materials & Processes

TABLE OF CONTENTS

	Page
INTRODUCTION	1
SPECIMEN AND MATERIAL	2
DISCUSSION OF THEORETICAL PREDICTIONS	6
Isotropic Hardening	9
Kinematic Hardening	10
Piecewise Linear Hardening	14
Anisotropy	18
Fracture	23
RESULTS	25
Isotropy	25
Initial Yielding	29
Strain Hardening	33
Fracture	42
CONCLUSIONS	44
REFERENCES	45

LIST OF FIGURES

Figure		Page
1	Sketch of Tubular Specimen.	3
2	Coordinate System.	4
3	Various Initial Yield Criteria in the Octahedral Plane.	8
4	Isotropic Hardening for Stress Path 01.	11
5	Kinematic Hardening for Stress Path 01.	15
6	Piecewise Linear Hardening for a Stress State Point in a Corner.	19
7	Piecewise Linear Hardening for a Stress State Point on AF.	20
8	Axial and Circumferential Plastic Strains in Pure Tension.	26
9	Specimen Adapted for Measurement of Internal Volume Change.	27
10	Volume Change in Internal Cavity of Tube.	28
11	Initial Yield Data at 78°F.	30
12	Initial Yield Data at 32°F.	32
13	Strain-Hardening Behavior, Test X-1. 78°F.	34
14	Strain-Hardening Behavior, Test X-3. 78°F.	35
15	Strain-Hardening Behavior, Test X-4. 78°F.	36
16	Strain-Hardening Behavior, Test X-9. 78°F.	37
17	Strain-Hardening Behavior, Test X-5. 32°F.	38
18	Strain-Hardening Behavior, Test X-6. 32°F.	39
19	Strain-Hardening Behavior, Test X-7. 32°F.	40
20	Strain-Hardening Behavior, Test X-8. 32°F.	41
21	Fracture Data for Combined Tension and Internal Pressure.	43

INTRODUCTION

The research reported here consisted of a theoretical and experimental investigation of the conditions for failure in cast zinc-alloy tubes at two testing temperatures.

This brings to an end one part of a general program, first, to examine the relationship of state of stress and temperature to failure of metals and, second, to develop failure criteria in terms of the macroscopic stresses, which has been in progress at The University of Michigan since 1958 under Air Force Contract No. AF 33(616)-6041. Previous work has been summarized in earlier reports.[1,2] Basically two types of material behavior are of concern in the general program:

1. Yielding followed by appreciable plastic deformation and terminating in ductile fracture.

2. Yielding followed by relatively little plastic deformation and terminating in brittle fracture.

The current research effort has related principally to three areas: (1) initial yielding, (2) changes in the conditions for continued plastic flow during strain hardening, and (3) rupture. From the theoretical viewpoint, the well-known theory of plasticity has been employed to define (or predict) an initial yield function or an initial yield surface in principal stress space. The motion of this yield surface during strain hardening has been examined in light of recent strain-hardening theories of plasticity. As has been noted in previous reports, the value of attempting to describe the material behavior in terms of the existing theory of plasticity is that techniques ° solution of boundary value problems already available could be used to extend the predictions of the theory to cases other than the simple one examined here. As regards rupture, the brittle nature of the fracture suggested that a criterion of the Griffith[3] type might be appropriate.

The experimental program has been planned to check some of the basic points which must be verified in order to use the available theory and to check predictions of the theory. It is not implied however that the yield conditions, flow rule, or stress-strain laws postulated in the theory of plasticity are intended to describe minutely the material behavior. The purpose of the experimental comparisons is to determine whether correct general trends are predicted by a theoretical model which is simple enough to be mathematically tractable in the solution of boundary value problems.

Manuscript released by the authors February 1962 for publication as a WADD Technical Documentary Report.

SPECIMEN AND MATERIAL

During the past year, attention has been centered on cast specimens of Zamak-3 zinc alloy, a material exhibiting the second type of behavior discussed in the Introduction. As noted in a previous report,[2] this material does undergo a "ductile to brittle" transition in that the principal strain at fracture changes from about 0.030 for the "ductile" state to about 0.007 or less for the "brittle" state. However the ultimate rupture appears to be transgranular and is not accompanied by localized plastic deformation processes, such as necking, in the separated region. Thus gross changes in the geometry of a tubular specimen do not occur. Two testing temperatures, 32°F and 78°F, were employed so that the range of states of stress for which brittle fracture occurred could be compared.

Details of casting procedure and composition have been reported previously.[2] It might be added here that no changes in the microstructure of a sample of this material have occurred since observations were begun in July, 1960.

The data reported herein were obtained by subjecting tubular specimens of the type shown in Figure 1 to various combinations of axial force and torque or axial force and internal pressure in a combined load testing machine. A complete description of the combined load testing machine is presented in WADD TR 60-234.[1] The ratio of axial force to torque can be held constant in this apparatus throughout a test run by a unique mechanico-hydraulic system. The thin walled tubular specimen has been used by many investigators. This sort of test specimen is advantageous since stresses are statically determinate to a good approximation for axial loading, torque, and internal pressure. In a material evaluation, it is of course essential that one be able to determine the state of stress directly from the applied loads without reference to the material properties.

In discussing the stresses in the tubular specimen it will be convenient to refer to the sketch of the coordinate system shown in Figure 2. For a test in which axial force and torque are applied, the stresses in the reduced section of the specimen are

$$\sigma_z = \frac{P}{2\pi rt}$$

$$\tau_{\theta z} = \frac{T}{2\pi r^2 t}$$

$$\sigma_r = \sigma_\theta = \tau_{r\theta} = \tau_{rz} = 0 \qquad (1)$$

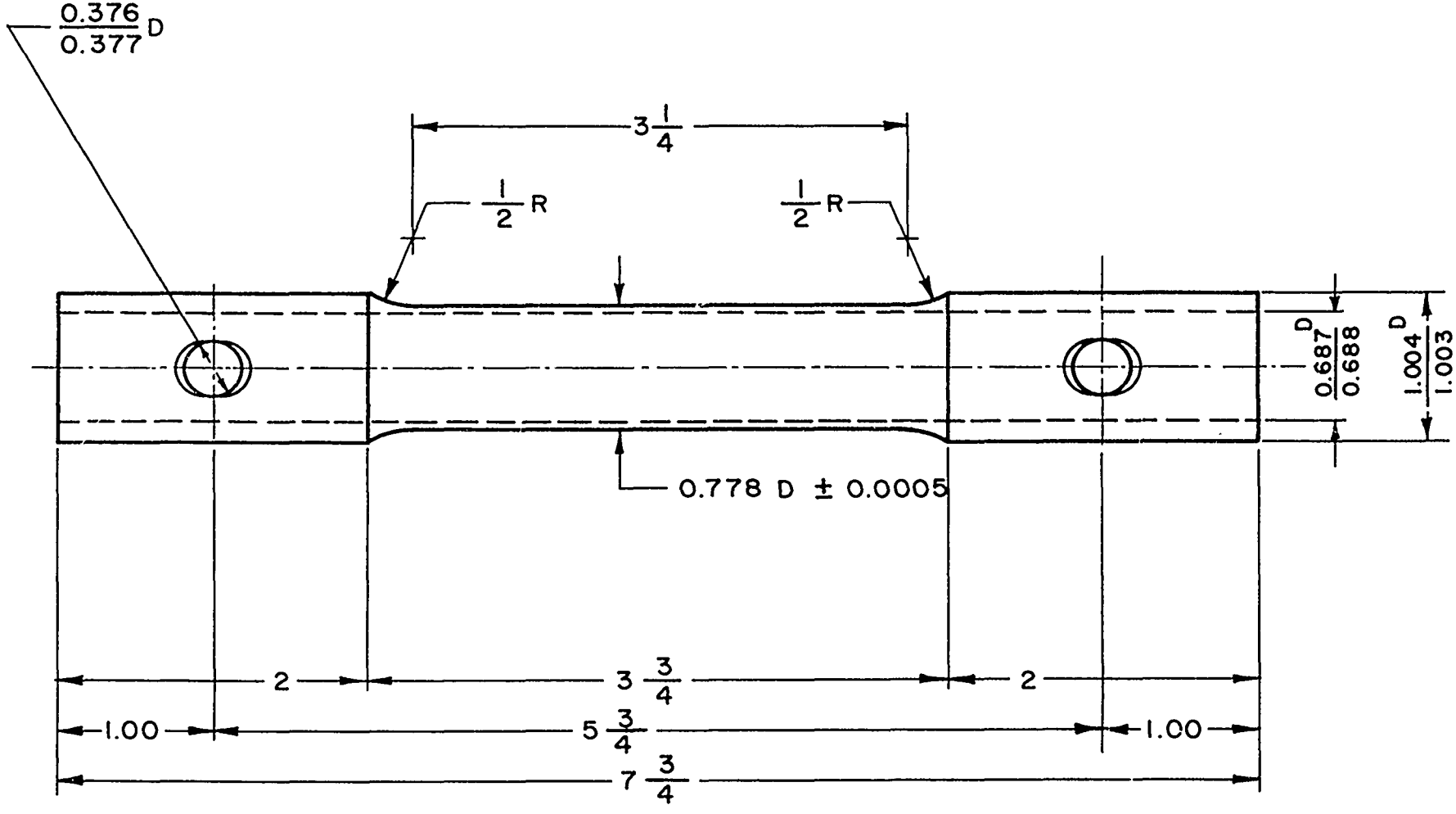

Figure 1. Sketch of Tubular Specimen.

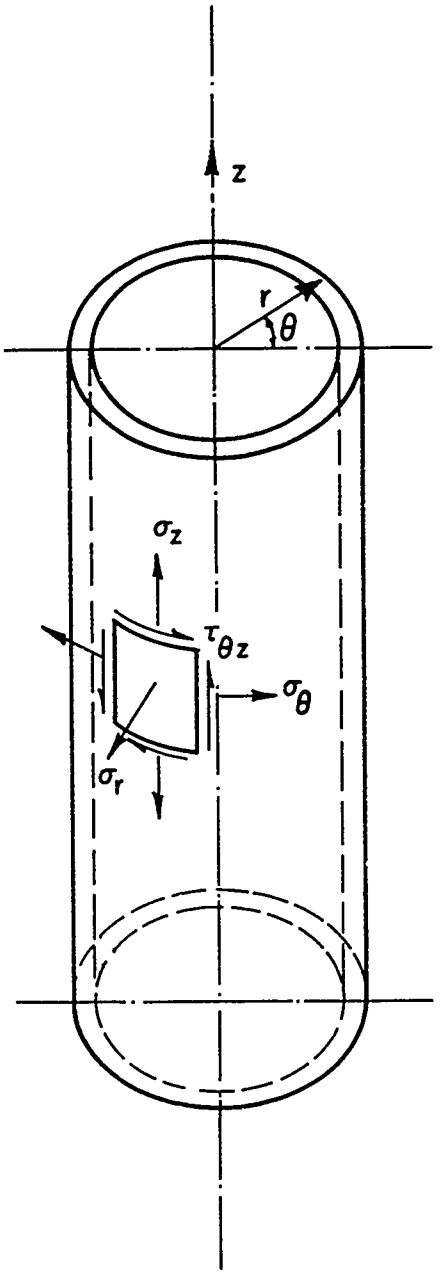

Figure 2. Coordinate System.

where:

r = mean radius of the reduced section
t = wall thickness
P = axial force
T = torque about z-axis.

Alternatively for a test combining axial force and internal pressure, the stresses are

$$\sigma_z = \frac{P}{2\pi rt} + \frac{pr}{2t}$$

$$\sigma_\theta = \frac{pr}{t}$$

$$\sigma_r = \tau_{r\theta} = \tau_{\theta z} = \tau_{rz} = 0. \qquad (2)$$

where p = internal pressure. In the above, stresses are computed in accordance with the usual assumptions for the membrane stresses in a thin-walled tube. For the tubes used,

$$\sigma_r \approx \frac{1}{8}\sigma_\theta$$

at the inner surface of the tube. This suggests that stress combinations where σ_z is much less than σ_θ be avoided since the assumption of $\sigma_r = 0$ relative to the other stress would not be acceptable in that case. Consequently, the smallest ratio used was $\sigma_z = 1/2\ \sigma_\theta$ which occurs for internal pressure alone.

In combined axial force and torque, σ_r is a principal stress since $\tau_{r\theta} = \tau_{rz} = 0$ and the principal directions lying in the θ-z plane depend on the ratio of σ_z to $\tau_{\theta z}$. The combined load testing machine should hold this ratio fixed in a given test and the principal directions should be fixed relative to an element of the material.

For combined axial force and internal pressure, the stresses σ_r, σ_θ, and σ_z are the principal stresses for all such load combinations since $\tau_{r\theta} = \tau_{\theta z} = \tau_{rz} = 0$ in all of them.

DISCUSSION OF THEORETICAL PREDICTIONS

The material model considered in this report is that of a rigid-strain hardening material. Here, rigid, refers to the fact that the theory deals only with the plastic portion of the total strain and thus all subsequent statements concerning strains relate to plastic strains. Further the model requires that states of stress which do not satisfy the yield condition or which lie inside the yield surface produce no (plastic) strain. When the stress state point reaches the yield surface, the yield surface moves in some prescribed manner corresponding to strain hardening and in addition (plastic) strains are produced.

If the material is assumed to be isotropic initially, the reference directions may be chosen at random and the principal directions of stress may be selected for convenience. Thus yield conditions may be stated in terms of the principal stresses and the yield surface may be considered in a space where the coordinates are the principal stresses σ_1, σ_2, and σ_3. Now further assume that yielding is independent of the average normal stress or mean stress defined by

$$\sigma = \frac{\sigma_1 + \sigma_2 + \sigma_3}{3} . \tag{3}$$

In this instance the yield stresses in tension and compression are the same. Further, the yield condition can be expressed as a function of the invariants of the stress deviator tensor, $F(J_2,J_3) = k^2$ and the yield surface in principal stress space is a cylinder with generators parallel to the octahedral ($\sigma_1 = \sigma_2 = \sigma_3$) axis. The latter point follows from the observation that a hydrostatic state of stress does not produce yielding.

In view of the above, any octahedral plane ($\sigma_1+\sigma_2+\sigma_3$ = constant) having a normal extending in the direction of the octahedral axis, would cut the yield surface at right angles. Further each intersection of octahedral plane and yield surface would be identical so any octahedral plane may be used. Thus in subsequent analysis the octahedral plane will be used to present results in a simple but general way.

Finally if a stable plastic material is assumed then the yield surface must be convex in accord with the "fundamental postulate" due to Drucker.[4] For convex yield surfaces, it can be shown that the strain increment vector must be normal to the yield surface which gives the flow rule of von Mises[5]

$$d\epsilon_{ij} = \lambda \frac{\partial F}{\partial \sigma_{ij}} \tag{4}$$

where $d\epsilon_{ij}$ is the plastic strain increment, $F(\sigma_{ij})$ is the yield function, and σ_{ij} is the stress. The flow rule will give the result that

$$d\epsilon_1 + d\epsilon_2 + d\epsilon_3 = 0 \tag{5}$$

for any yield condition which is independent of mean stress. Since the strain-increment vector is normal to the yield surface it would be expected to lie in an octahedral plane.

To demonstrate the use of the octahedral plane, several initial yield criteria consistent with the preceding restrictions are shown plotted on the octahedral plane in Figure 3. The circle corresponds to the von Mises condition for initial yielding,

$$(\sigma_1 - \sigma_2)^2 + (\sigma_2 - \sigma_3)^2 + (\sigma_3 - \sigma_1)^2 = 2\sigma_0^2 \tag{6}$$

where σ_0 is the yield stress in simple tension or compression. The radius of this circle in the octahedral plane is $\sqrt{2/3}\ \sigma_0$. Hexagon ABCDEFA corresponds to the Tresca initial yielding condition

$$\max\{|\sigma_1 - \sigma_2|, |\sigma_2 - \sigma_3|, |\sigma_3 - \sigma_1|\} = \sigma_0 \tag{7}$$

A new yield criterion called the maximum reduced stress criterion has been proposed by Haythornthwaite[6] and may be stated as follows

$$\max\{|\sigma_1 - \sigma|, |\sigma_2 - \sigma|, |\sigma_3 - \sigma|\} = \frac{2}{3}\sigma_0 \tag{8}$$

where σ is the average normal stress or mean stress. This criterion states that yielding occurs when the absolute value of the largest principal stress deviator reaches a limiting value. It is represented by the external hexagon GHIJKLG. The choice of pure tension as a point of agreement between the various theories was arbitrary.

Treating σ_3 as σ_r, the range of stress combinations easily obtainable in the combined load testing machine lie in the lesser angle LOH in Figure 3.

As noted already yielding begins when the stress state point reaches one of these yield surfaces and plastic straining continues as long as the state point tends to cause outward motion of the yield surface. Several theories

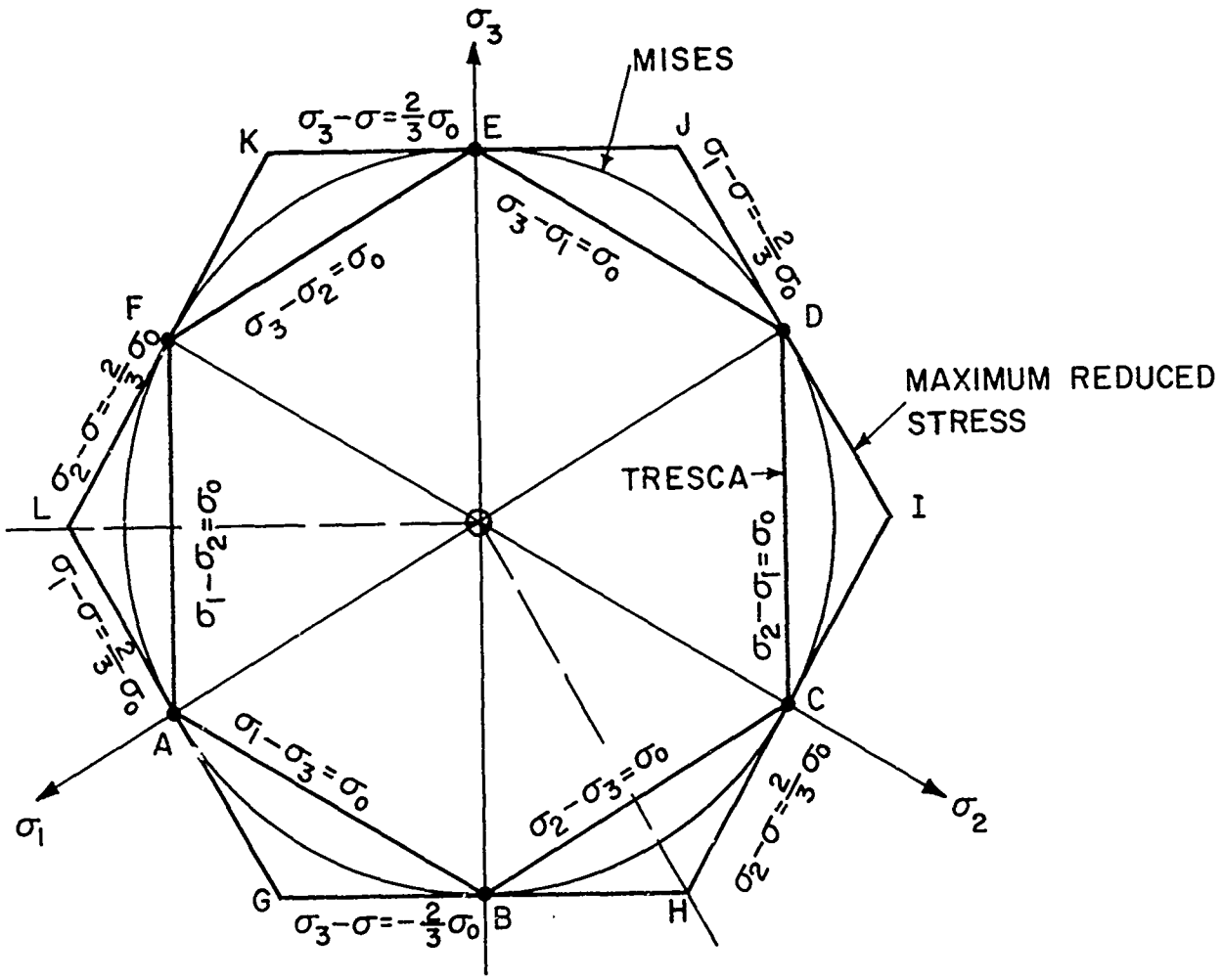

Figure 3. Various Initial Yield Criteria in the Octahedral Plane.

of strain hardening will be used to predict motions of the yield surface during this process.

ISOTROPIC HARDENING

Isotropic hardening, as presented by Hill,[7] postulates that the yield surface enlarges in a symmetrical manner with respect to the origin during plastic straining or strain hardening. Thus the initial yield surface

$$F(\sigma_{ij}) = k^2 \tag{9}$$

becomes

$$F(\sigma_{ij}) = c^2 \geq k^2 \tag{10}$$

after hardening. Obviously no Bauschinger effect is considered. To obtain a stress increment-strain increment relationship note that when the stress state point moves on the yield surface, $dF = 0 = \partial F/\partial\sigma_{ij}\ (d\sigma_{ij})$ and there is no plastic strain in this instance suggesting for $dF > 0$ the form

$$d\epsilon_{ij} = G_{ij}dF. \tag{11}$$

Now by use of the flow rule we obtain

$$d\epsilon_{ij} = Q\,\frac{\partial F}{\partial\sigma_{ij}} \cdot \frac{\partial F}{\partial\sigma_{k\ell}}\,d\sigma_{k\ell} \tag{12}$$

where, as usual, repeated subscripts denote summation, and Q is a scalar which may depend on stress, strain, and their histories.

As an example, consider the Tresca yield criterion. Incidentally, the Tresca criterion has the distinct advantage that the plastic strain increments are partially independent of the stress path. For a stress state point in contact with side AB, the stress-strain laws or flow laws for side AB where $F = \sigma_1 - \sigma_3 = \sigma_0$ are

$$\begin{aligned} d\epsilon_1 &= Q(d\sigma_1 - d\sigma_3) \\ -d\epsilon_3 &= Q(d\sigma_1 - d\sigma_3) \\ d\epsilon_2 &= 0 \end{aligned} \tag{13}$$

In the preceding, $d\sigma_1$, $d\sigma_2$, and $d\sigma_3$ represent the incremental changes in the principal stress components as the stress state point proceeds beyond the initial yield surface. According to the isotropic hardening theory, side AB moves in the direction of the outward normal a distance proportional to $(d\sigma_1 - d\sigma_3)$ and the other sides will move the same distance along their outward normals.

The corresponding flow laws for the Mises criterion are considerably more complex but the geometric interpretation of the influence of a stress point moving away from the origin is similar to the above.

Considering now an example involving the maximum reduced stress criterion, the flow laws for a stress state point on side LG would be

$$d\epsilon_1 = Q(2/9)(2d\sigma_1 - d\sigma_2 - d\sigma_3)$$

$$d\epsilon_2 = Q(-1/9)(2d\sigma_1 - d\sigma_2 - d\sigma_3)$$

$$d\epsilon_3 = Q(-1/9)(2d\sigma_1 - d\sigma_2 - d\sigma_3) \qquad (14)$$

As with the Tresca criterion, the plastic strain increments are partially independent of the stress path. Motion of the side LG during hardening would be along the outward normal in an amount which is proportional to $(2/3\ \sigma_1 - 1/3\ \sigma_2 - 1/3\ \sigma_3)$ and by the isotropic hardening hypothesis the other sides move outward like amounts.

Figure 4 presents geometrically a typical prediction of isotropic hardening theory for the stress path 01. The solid circles and hexagons represent the final positions of the various yield surfaces or loading surfaces presuming loading is stopped at point 1. If, as suggested earlier, σ_3 is treated as σ_r, then $\sigma_1 = \sigma_z$ and $\sigma_2 = \sigma_\theta$ and the path 01 would be produced by a combination of axial tensile force and internal pressure. By considering various stress paths on Figure 4, one can easily show that the final position of the yield surface depends only on the final state of plastic strain and not on the path.

KINEMATIC HARDENING

The kinematic theory of hardening originally proposed by Prager and delineated by Shield and Ziegler,[9] states that the initial yield surface

$$F(\sigma_{ij}) = k^2 \qquad (15)$$

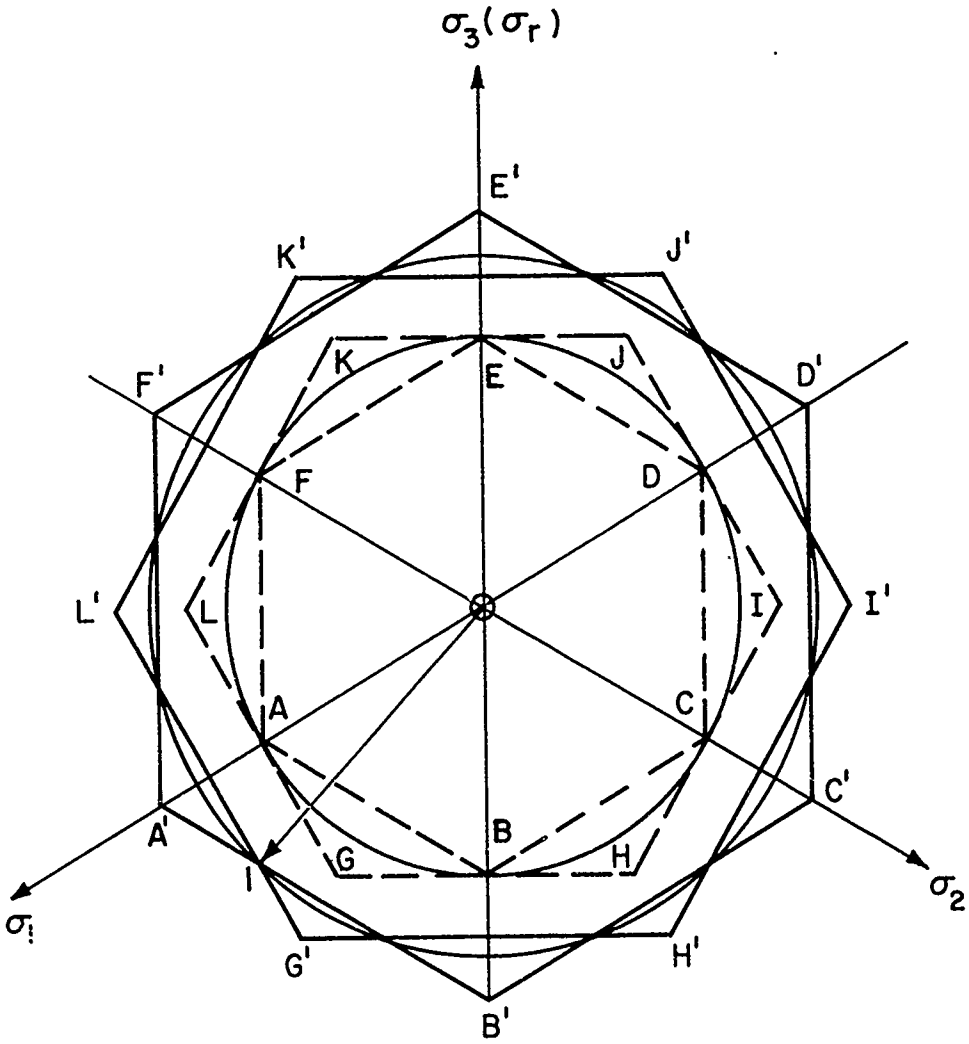

Figure 4. Isotropic Hardening for Stress Path 01.

becomes, after hardening

$$F(\sigma_{ij} - \alpha_{ij}) = k^2 . \tag{16}$$

The flow rule is assumed to apply and the yield surface is assumed to translate without changing the form of $F(\sigma_{ij})$. The tensor α_{ij} represents the translation of the yield surface which occurs in the direction of $d\epsilon_{ij}$ (i.e., the outward drawn normal to the yield surface). Thus

$$d\alpha_{ij} = c d\epsilon_{ij} . \tag{17}$$

This strain hardening theory gives predictions of material behavior which include the Bauschinger effect.

For this theory, the condition that the stress state point must remain on the translating yield surface leads to the requirement that

$$(d\sigma_{ij} - d\alpha_{ij}) \frac{\partial F}{\partial \sigma_{ij}} = 0 . \tag{18}$$

Combining this with the equation for $d\alpha_{ij}$ and the flow rule gives, during loading

$$d\epsilon_{ij} = \frac{1}{c} \cdot \frac{1}{\frac{\partial F}{\partial \sigma_{mn}} \cdot \frac{\partial F}{\partial \sigma_{mn}}} \cdot \frac{\partial F}{\partial \sigma_{ij}} \cdot \frac{\partial F}{\partial \sigma_{k\ell}} \cdot d\sigma_{k\ell} . \tag{19}$$

This is similar to the stress increment-strain increment relation developed earlier in isotropic hardening, indicating a linear relationship between the two.

Since α_{ij} is not necessarily an isotropic tensor (i.e., components invariant with rotation) it is expected that an initially isotropic material may become anisotropic with strain hardening. Consider the case in which the principal axes of the stress tensor are fixed in an element of the material during plastic straining. These principal axes can then be treated as the reference axes. For an initially isotropic material $\alpha_{ij} = 0$ and the flow rule gives the information that

$$d\epsilon_{ij} = 0 \quad (i \neq j) \tag{20}$$

since the principal axes of stress and strain increment tensors coincide. The above equation woulo not be correct if the reference axes were not the principal axes of stress during the initial strain increment. It follows that

$$d\alpha_{ij} = 0 \quad (i \neq j) \tag{21}$$

under these conditions and principal axes of stress remain principal axes during hardening.

Referring to the previous section, it is noted that the principal axes of stress in the tubular specimens are fixed in an element of the material for all combinations of axial force and internal pressure. For axial force and torque, the principal axes of stress are also fixed as long as the control system maintains a constant ratio of axial force to torque.

For convenience, let us state the kinematic hardening theory in terms of the principal stresses as follows:

$$F(\sigma_1, \sigma_2, \sigma_3) = k^2 \tag{22}$$

before hardening becomes

$$F[(\sigma_1 - c\epsilon_1), (\sigma_2 - c\epsilon_2), (\sigma_3 - c\epsilon_3)] = k^2 \tag{23}$$

after hardening. The quantities $c\epsilon_1$, $c\epsilon_2$, and $c\epsilon_3$ represent the translation of the yield surface as a rigid body in principal stress space, the translation occurring in the direction of the outward normal to the yield surface at the stress state point.

For demonstrative purposes, again consider the example of a situation where the Tresca theory applies and the stress state point remains on side AB as indicated in Figure 3. The stress-strain laws or flow laws have the same form

$$\begin{aligned} d\epsilon_1 &= 1/2c\ (d\sigma_1 - d\sigma_3) \\ -d\epsilon_3 &= 1/2c\ (d\sigma_1 - d\sigma_3) \\ d\epsilon_2 &= 0. \end{aligned} \tag{24}$$

During loading it can be shown that the center of the hexagon ABCDEFA in Figure 3 moves an amount $1/\sqrt{2}\ (d\sigma_1 - d\sigma_3)$ in a direction perpendicular to AB. When $\sigma_3 = \sigma_r$, $\sigma_1 = \sigma_z$ and $\sigma_2 = \sigma_\theta$, this is what might occur for loading caused by combined axial tension and internal pressure. Should the stress state point enter a corner of the Tresca hexagon, the yield surface will move in the direction of the stress increment vector.

When the maximum reduced stress criterion applies and side LG is contacted by the stress state point, the flow laws are the same as those given for the case under isotropic hardening except that $Q = 3/2c$. The entire hexagon GHIJKLG in Figure 3 moves as a unit an amount $1/\sqrt{6}\ (2/3\ \sigma_1 - 1/3\ \sigma_2 - 1/3\ \sigma_3)$ along a line perpendicular to LG.

Figure 5 shows the motions of the various yield surfaces for kinematic hardening under stress path 01. The solid circle represents the final position for the Mises criterion, the solid hexagon A'B'C'D'E'F'A' represents the final position for the Tresca criterion, and G'H'I'J'K'L'G' the final position for the maximum reduced stress criterion. The vector 02 denotes the motion of the Tresca hexagon or $1/\sqrt{2}\ (d\sigma_1 - d\sigma_3)$. Similarly the vector 03 represents the motion of the Mises circle. Finally the vector 04 of magnitude $1/\sqrt{6}\ (2/3\sigma_1 - 1/3\sigma_2 - 1/3\sigma_3)$ gives the motion of the center of the hexagon representing the maximum reduced stress criterion. As above, a stress state point entering a corner will cause a motion of the yield surface in the direction of the stress increment vector. The forms for the various yield criteria after kinematic hardening are:

Mises

$$[(\sigma_1 - \sigma_3) - c(\epsilon_1 - \epsilon_3)]^2 + [(\sigma_1 - \sigma_2) - c(\epsilon_1 - \epsilon_2)]^2 + [(\sigma_2 - \sigma_3) - c(\epsilon_2 - \epsilon_3)]^2 = 2\sigma_0^2$$

Tresca

$$\max\{|\sigma_1 - \sigma_2 - c(\epsilon_1 - \epsilon_2)|,\ |\sigma_1 - \sigma_3 - c(\epsilon_1 - \epsilon_3)|,\ |\sigma_2 - \sigma_3 - c(\epsilon_2 - \epsilon_3)|\} = \sigma_0$$

Maximum Reduced Stress

$$\max\{|\sigma_1 - \sigma - c\epsilon_1|,\ |\sigma_2 - \sigma - c\epsilon_2|,\ |\sigma_3 - \sigma - c\epsilon_3|\} = \frac{2}{3}\sigma_0 \qquad (25)$$

PIECEWISE LINEAR HARDENING

A third strain-hardening theory has been developed by Hodge[10] and is referred to here as piecewise linear hardening. Hodge's work is based solely on the Tresca yield criterion and takes advantage of the limited stress path independence of such a criterion. This theory differs from the isotropic or kinematic hardening theories in that relative motions between the sides of the yield surface during plastic straining are permitted, whereas the yield sur-

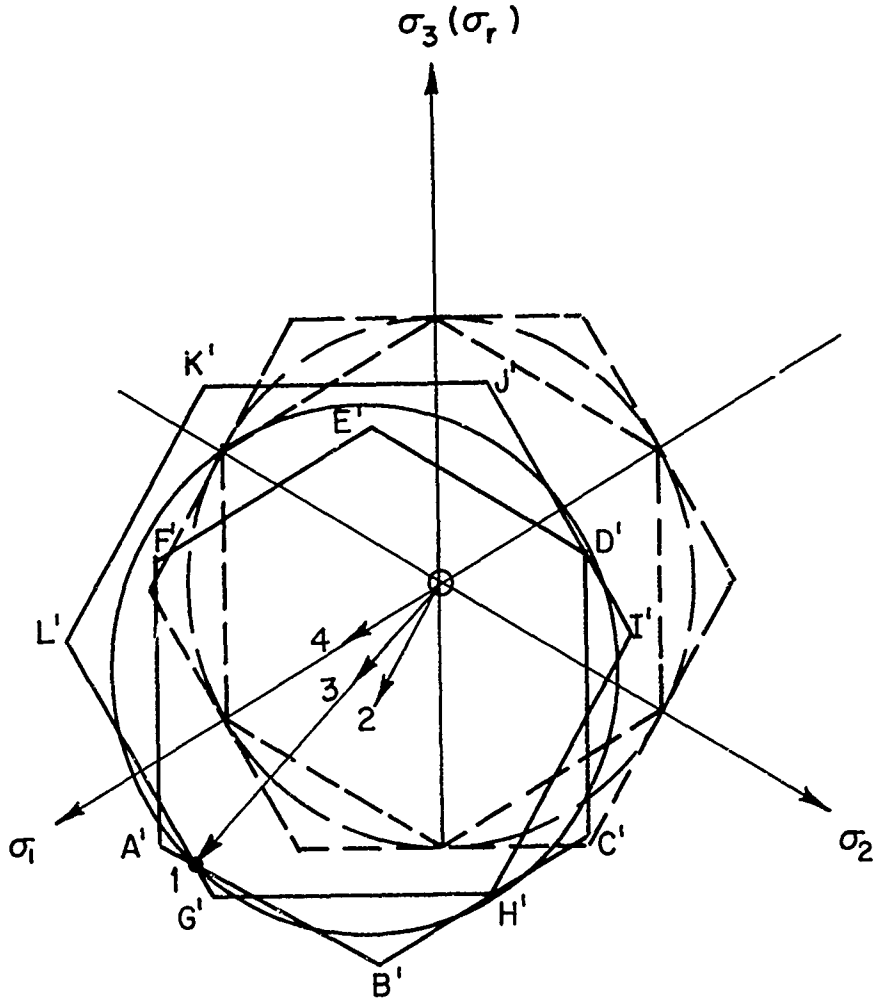

Figure 5. Kinematic Hardening for Stress Path 01.

face moves as a rigid body in kinematic hardening and merely enlarges for isotropic hardening. Sanders[11] suggested earlier the idea of using a yield surface having a finite number of plane sides but the theory was not fully developed. In Hodge's theory, rotation of sides of the yield surface, formation of sides, or disappearance of sides is not permitted. Although the sides may move independently, the only permissible motions are pure translations. Principal axes of stress and strain must coincide and remain fixed in an element of the material throughout the plastic straining process.

The theory is developed by establishing flow laws for all of the sides of the yield surface, first for a stress state point in contact with a selected side and then for a stress state point in a corner of the yield surface. Again refer to Figure 3.

Suppose first that the stress state point remains on side AF, where $F = \sigma_1 - \sigma_2 = \sigma_0$. The flow laws are

$$d\epsilon_1 = 1/2c\ (d\sigma_1 - d\sigma_2)$$

$$-d\epsilon_2 = 1/2c\ (d\sigma_1 - d\sigma_2)$$

$$d\epsilon_3 = 0. \tag{26}$$

As for the Tresca criterion in kinematic hardening, the motion of side AF is then $1/\sqrt{2}\ (d\sigma_1 - d\sigma_2)$ or $\sqrt{2}\ c d\epsilon$. For convenience the symbol K will be substituted for $\sqrt{2}\ c$ hereafter. The motion of side AF is now stated as

$$Kd\epsilon_1 = 1/\sqrt{2}\ (d\sigma_1 - d\sigma_2). \tag{27}$$

Now consider motion of the other sides while the stress state point remains on AF. Side AB may move an amount proportional to the motion of AF so that its movement along its normal is given by

$$\alpha Kd\epsilon_1 = 1/\sqrt{2}\ (d\sigma_1 - d\sigma_3). \tag{28}$$

The side EF would move an equal distance along its normal so that

$$\alpha Kd\epsilon_1 = 1/\sqrt{2}\ (d\sigma_3 - d\sigma_2). \tag{29}$$

Side BC may move independently but still an amount proportional to that of AF resulting in

$$\beta K d\epsilon_1 = 1/\sqrt{2}\,(d\sigma_2 - d\sigma_3). \tag{30}$$

Side DE moves a like amount to BC so that

$$\beta K d\epsilon_1 = 1/\sqrt{2}\,(d\sigma_3 - d\sigma_1). \tag{31}$$

Now side CD may also be independent so its motion is

$$\gamma K d\epsilon_1 = 1/\sqrt{2}\,(d\sigma_2 - d\sigma_1). \tag{32}$$

To prevent disappearance of sides, Hodge[10] shows that

$$-2\beta \leqq -\gamma \leqq \alpha - \beta \leqq 1 \leqq 2\alpha. \tag{33}$$

The above will coincide with the predictions of the kinematic theory if $\alpha = 1/2$, $\beta = -1/2$, and $\gamma = -1$ and will coincide with the isotropic theory if $\alpha = \beta = \gamma = 1$.

To indicate the significance of the quantities α, β, γ the behavior of the yield surface for a stress state point entering a corner must be known. This however requires consideration of the motions under another side regime. If the stress state point lies on side AB, where $\sigma_1 - \sigma_3 = \sigma_o$, the flow law and side motion for this side is

$$K d\epsilon_1 = 1/\sqrt{2}\,(d\sigma_1 - d\sigma_3) = -K d\epsilon_3. \tag{34}$$

Now for this case, adjacent side AF moves along its outward normal the distance

$$\alpha K d\epsilon_1 = 1/\sqrt{2}\,(d\sigma_1 - d\sigma_2). \tag{35}$$

Finally let the stress state point enter corner A as in Figure 6. In this instance, sides AB and AF are both moved directly by the stress state point. Note that for a stress state point on AF, $d\epsilon_1 = -d\epsilon_2$, while for a stress state point on AB, $d\epsilon_1 = -d\epsilon_3$. Then superpose the two simultaneous motions using the expressions just given and obtain flow laws for AB

$$1/\sqrt{2}\,(d\sigma_3 - d\sigma_1) = Kd\epsilon_3 + \alpha Kd\epsilon_2 \tag{36}$$

and for AF

$$1/\sqrt{2}\,(d\sigma_2 - d\sigma_1) = Kd\epsilon_2 + \alpha Kd\epsilon_3. \tag{37}$$

The boundary line between side regime, say AF, and corner regime, say A, is defined by considering a stress state point on the boundary. If the state point is considered as being on side AF, $d\epsilon_3 = 0$. Using this information in the above flow laws, since the state point is also in the corner, we obtain

$$d\sigma_1 - d\sigma_3 = \alpha(d\sigma_1 - d\sigma_2). \tag{38}$$

Thus α is the ratio of adjacent side motions when the stress state point is on the boundary. When α is known, a stress state point can be established as being on side AF if $d\sigma_1 - d\sigma_3 < \alpha(d\sigma_1 - d\sigma_2)$ and as being in corner A if $d\sigma_1 - d\sigma_3 > \alpha(d\sigma_1 - d\sigma_2)$. If the stress state point is on side AF, corner A follows the boundary defined by $d\sigma_1 - d\sigma_3 = \alpha(d\sigma_1 - d\sigma_2)$.

Figure 7 presents the motions of the sides of the yield surface for a stress state point which remains on side AF and for $\alpha = 0.6$, $\beta = 0$, and $\gamma = -0.3$. The indicated stress path 01 is a radial one although it is not necessary to these motions of the yield surface that a radial path be maintained as long as the state point is always on AF. It is apparent that a similar theory could be developed using the maximum reduced stress criterion in place of Tresca.

ANISOTROPY

Since one of the functions of the experimental program is to establish the isotropy or lack of it of the Zamak-3 tubes, the nature of the anisotropy that might appear will be considered.

Hill[12] has suggested an analysis for a particularly simple type of anisotropy and the following is adapted from his analysis.

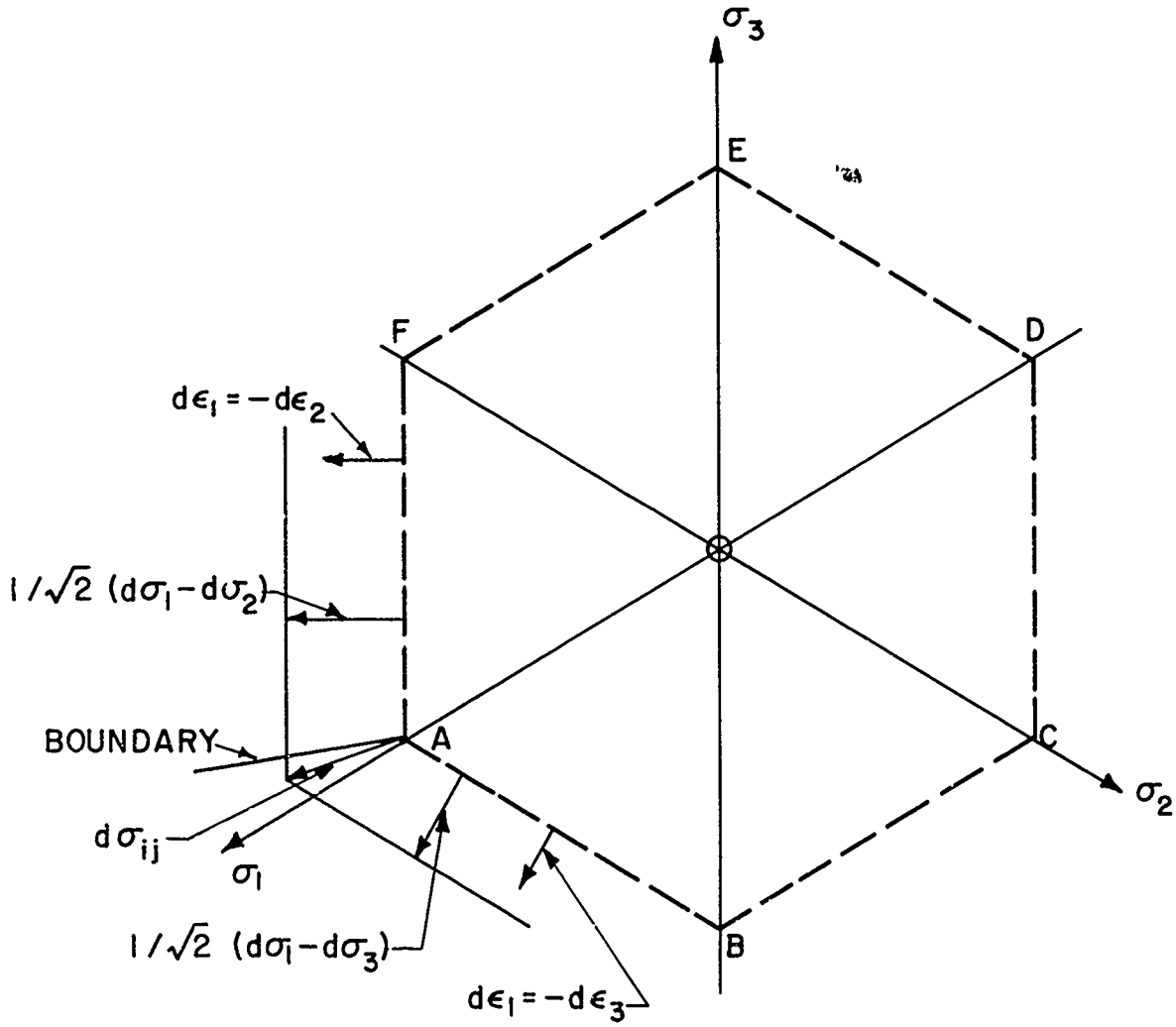

Figure 6. Piecewise Linear Hardening for a Stress State Point in a Corner.

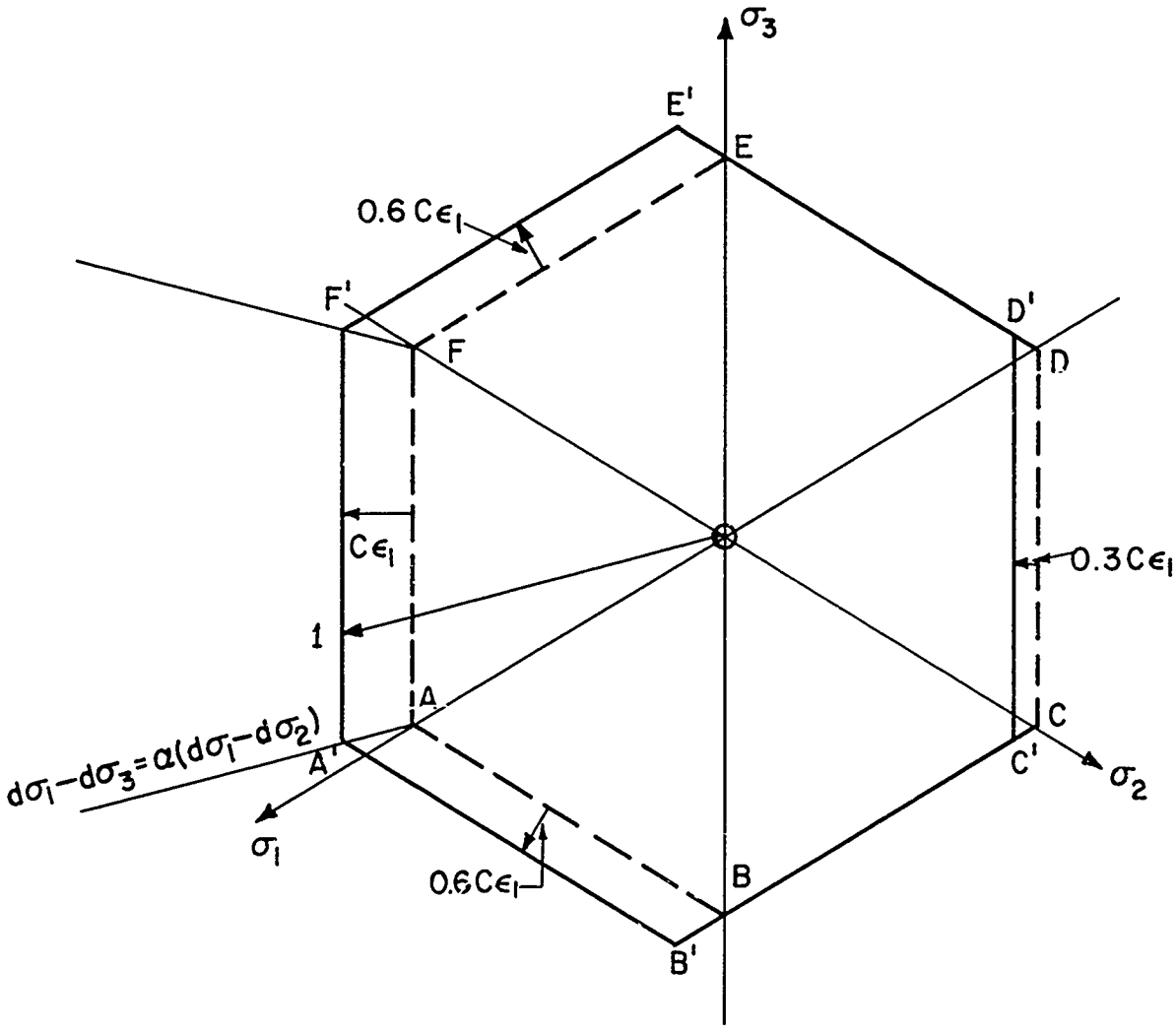

Figure 7. Piecewise Linear Hardening for a Stress State Point on AF.

First assume that the principal axes of anisotropy in cast Zamak-3 tubes are the r-, θ- and z-axes (see Figure 2). Further assume that yielding in the material remains insensitive to mean stress and that the general form of the Mises yield criterion is applicable. A yield function in accord with these assumptions is

$$F(\sigma_\theta-\sigma_z)^2 + G(\sigma_z-\sigma_r)^2 + H(\sigma_r-\sigma_\theta)^2 + 2L\tau_{\theta z}^2 + 2M\tau_{rz}^2 + 2N\tau_{r\theta}^2 = 1. \quad (39)$$

The constants F, G, and H are related to the yield stresses σ_r^*, σ_θ^*, σ_z^*, in the r-, θ- and z-directions as follows:

$$\frac{1}{(\sigma_r^*)^2} = G+H; \quad \frac{1}{(\sigma_\theta^*)^2} = H+F; \quad \frac{1}{(\sigma_z^*)^2} = F+G. \quad (40)$$

Similarly

$$2L = \frac{1}{(\tau_{\theta z}^*)^2}; \quad 2M = \frac{1}{(\tau_{rz}^*)^2}; \quad 2N = \frac{1}{(\tau_{r\theta}^*)^2}; \quad (41)$$

for the yield stresses in shear relative to the principal axes.

It would appear that a particular type of anisotropy which might occur in cast material would be characterized by rotational symmetry of anistropy about the r-axis. This means that the yield stresses in θ and z-directions would be equal. Since the Zamak-3 specimens were cast as solid cylindrical bars, it is possible that slight radial variations in grain structure might occur as a result of the varying rate of cooling in the radial direction. Such as situation could lead to the type of anisotropy described.

Now if one restricts the values of the constants in the above yield function so that isotropy is present for a rotation of the coordinate system about the r-axis, the following relationships result:

$$H = G$$

$$2F + H = L$$

$$M = N. \quad (42)$$

The yield function then becomes

$$F(\sigma_\theta-\sigma_z)^2 + H(\sigma_z-\sigma_r)^2 + H(\sigma_r-\sigma_\theta)^2 + 2(2F+H)\tau_{\theta z}^2 + 2M\tau_{rz}^2 + 2M\tau_{r\theta}^2 = 1. \tag{43}$$

Applying the flow rule, the following plastic strain increments are obtained:

$$\begin{aligned}
d\epsilon_z &= \lambda[2F(\sigma_z-\sigma_\theta) + 2H(\sigma_z-\sigma_r)] \\
d\epsilon_\theta &= \lambda[2F(\sigma_\theta-\sigma_z) + 2H(\sigma_\theta-\sigma_r)] \\
d\epsilon_r &= \lambda[2H(2\sigma_r-\sigma_\theta-\sigma_z)] \\
d\gamma_{\theta z} &= \lambda \cdot 4(2F+H)\tau_{\theta z} \\
d\gamma_{rz} &= \lambda \cdot 4M\tau_{rz} \\
d\gamma_{r\theta} &= \lambda \cdot 4M\tau_{r\theta} .
\end{aligned} \tag{44}$$

From the above it is easy to show that

$$d\epsilon_r + d\epsilon_\theta + d\epsilon_z = 0. \tag{45}$$

For a pure tension test where σ_z is the only non-zero stress, the ratio of circumferential plastic strain increment to axial plastic strain increment is

$$-\frac{d\epsilon_\theta}{d\epsilon_z} = \frac{F}{F+H} . \tag{46}$$

In totally isotropic material, the yield function is $F(J_2, J_3) = k^2$ if the yield is independent of mean stress. J_2 and J_3 as before are the invariants of the stress deviator tensor. The flow rule for this case gives

$$-\frac{d\epsilon_\theta}{d\epsilon_z} = \frac{1}{2} . \tag{47}$$

Thus a comparison of axial and circumferential plastic strains might detect the presence of a radially symmetric anisotropy.

It should be noted that a comparison of axial and circumferential strains in a tension test is equivalent to the measurement of internal volume change performed by Taylor and Quinney.[13] This permanent internal volume change for a tube is

$$\Delta V = \pi \ell r^2 (d\epsilon_z + 2d\epsilon_\theta). \tag{48}$$

For zero volume change in the internal cavity it is necessary that

$$d\epsilon_z = -2d\epsilon_\theta. \tag{49}$$

It follows that the type of anisotropy described above would cause a permanent change in volume of the internal cavity of a tube.

Pugh[14] notes that measurement of internal volume change can not detect the presence of anisotropy which is rotationally symmetric about the z-axis. While such anisotropy could be present in, say, cold-drawn tubes, it is not considered to be likely in cast tubes.

FRACTURE

Brittle fracture in materials of essentially zero ductility has been discussed by Griffith.[3] His theory assumes that the material is elastic at the instant of fracture or rupture which is brought on by the presence of small elliptical cracks or holes. The theoretical work applies only to instances of plane stress and thus would apply only to bodies having one dimension small relative to the others. It is postulated that rupture occurs when the largest stress tangent to the most favorably oriented ellipse reaches a limiting value. This assumes that there are a sufficient number of pre-existing cracks or ellipses so that some ellipse will always be in the most favorable orientation. By relating this maximum stress to the applied plane principal stresses the following is obtained:

$$\text{a.} \quad \text{If } 3\sigma_1 + \sigma_2 > 0 \text{ then } \sigma_1 = \sigma_r \tag{50}$$

where σ_r is the rupture stress in say tension for a particular material,

$$\text{b.} \quad \text{If } 3\sigma_1 + \sigma_2 < 0 \text{ then } (\sigma_1 - \sigma_2)^2 + 8\sigma_r(\sigma_1 + \sigma_2) = 0. \tag{51}$$

In the above σ_1 is algebraically larger than σ_2 in all cases.

The above criteria indicate that the test conditions prevalent in this program, ranging from pure internal pressure to pure torsion, all fall within category a. Category a is, in effect, a maximum normal stress criterion of rupture.

RESULTS

During the past year, a considerable body of experimental data have been accumulated which can now be used to test the theoretical predictions just discussed. In considering the experimental data at least two things should be borne in mind.

1. Scatter in properties from specimen to specimen of Zamak-3 is known to exist.

2. None of the theories discussed previously will furnish exact predictions of material behavior.

ISOTROPY

In the previous section, it is shown that an isotropic tube under tension along the z-axis should exhibit a ratio of circumferential plastic strain to axial plastic strain of -1/2. Total plastic strains can be considered rather than plastic strain increments because the stress path is a radial one.

Figure 8 presents a plot of axial plastic strain against circumferential plastic strain for two tension tests. The test data marked OP-12 were obtained at 78°F and the test data marked OP-14 were obtained at 32°F. Strains were measured with foil strain gages attached with Eastman 910 cement. For OP-12 the ratio of circumferential plastic strain to axial plastic strain is 0.53 while for OP-14 the ratio is 0.54. This indicates a very slight, if any, anisotropy.

A test of plastic volume change in the internal cavity of the specimen, somewhat similar to that of Taylor and Quinney, was also performed at a testing temperature of 32°F. Figure 9 is a sketch of a specimen with rubber plugs and plastic tubing in place. The volume change which was measured is that lying between the two rubber plugs. This region and the tubing was filled with water and permitted to stand overnight. During loading, the change in water level was measured on a scale at roughly the same height as the specimen itself. Of course this apparatus measures both elastic and plastic volume change in the internal cavity. To evaluate the plastic volume change, in Figure 10 a plot is made of the actual or measured volume change against the computed elastic volume change. In a tension test the elastic volume change in the internal cavity is given by

$$\Delta V = \pi r^2 \ell (1-2\nu)\frac{\sigma_z}{E} \tag{52}$$

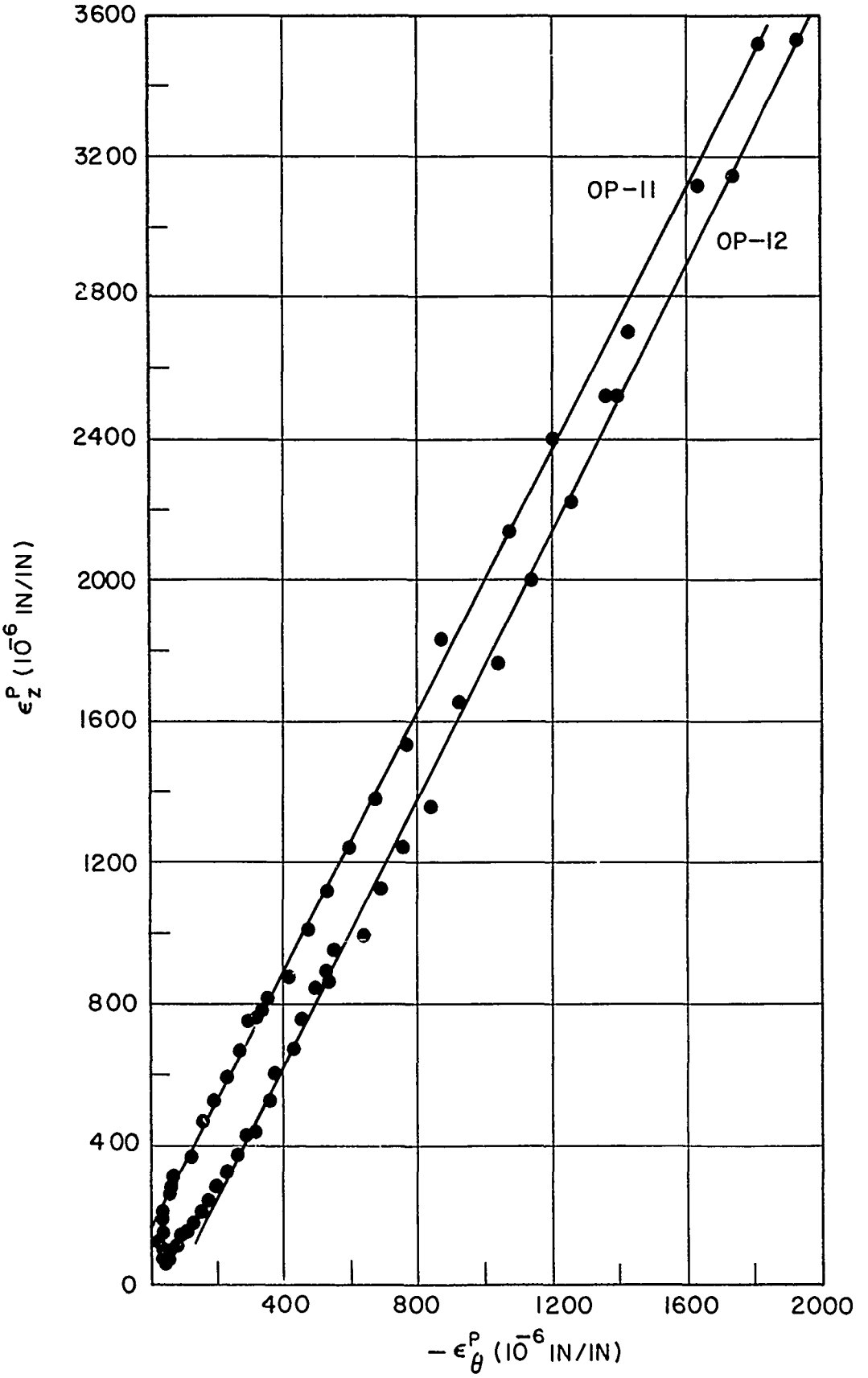

Figure 8. Axial and Circumferential Plastic Strains in Pure Tension.

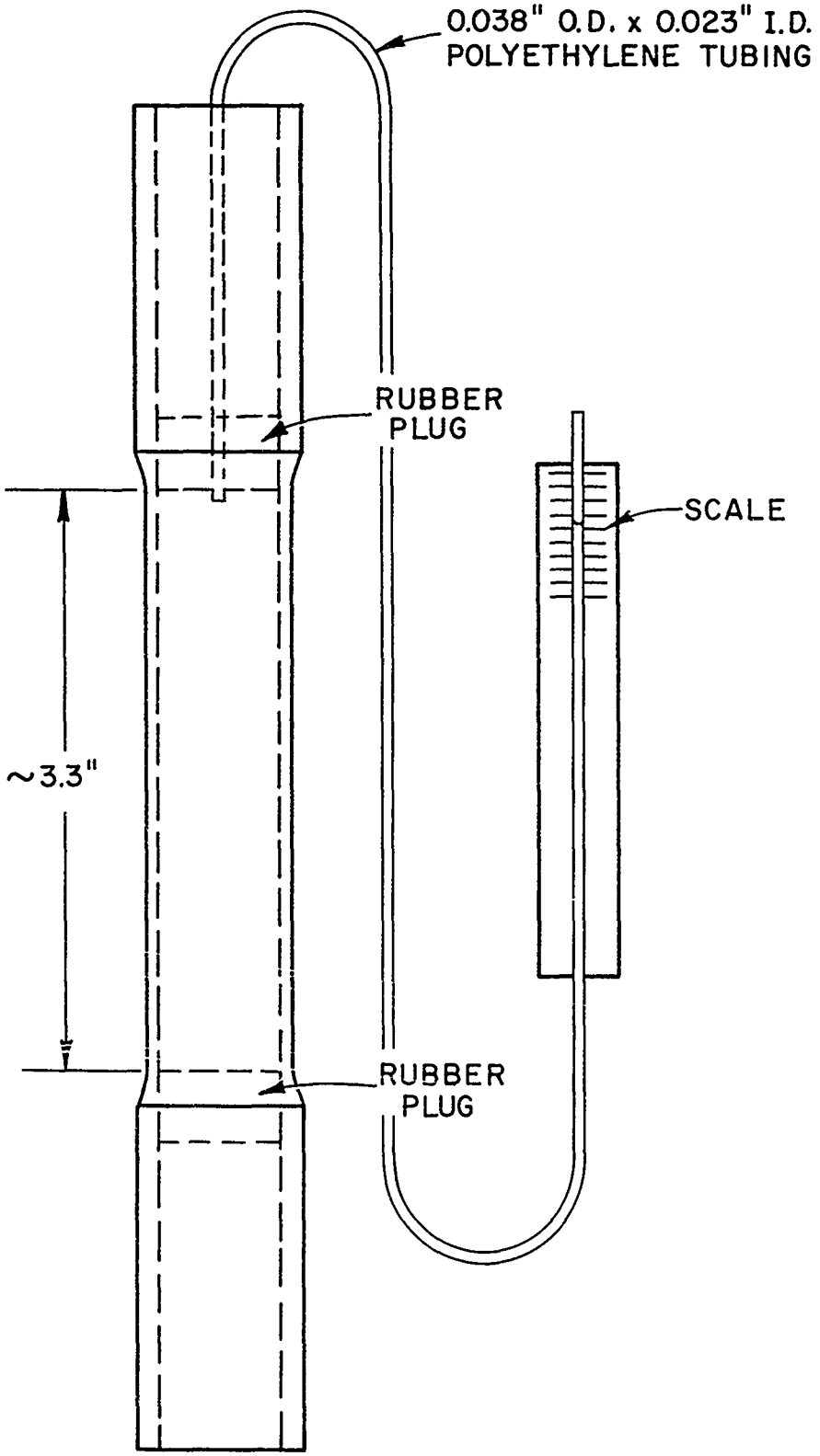

Figure 9. Specimen Adapted for Measurement of Internal Volume Change.

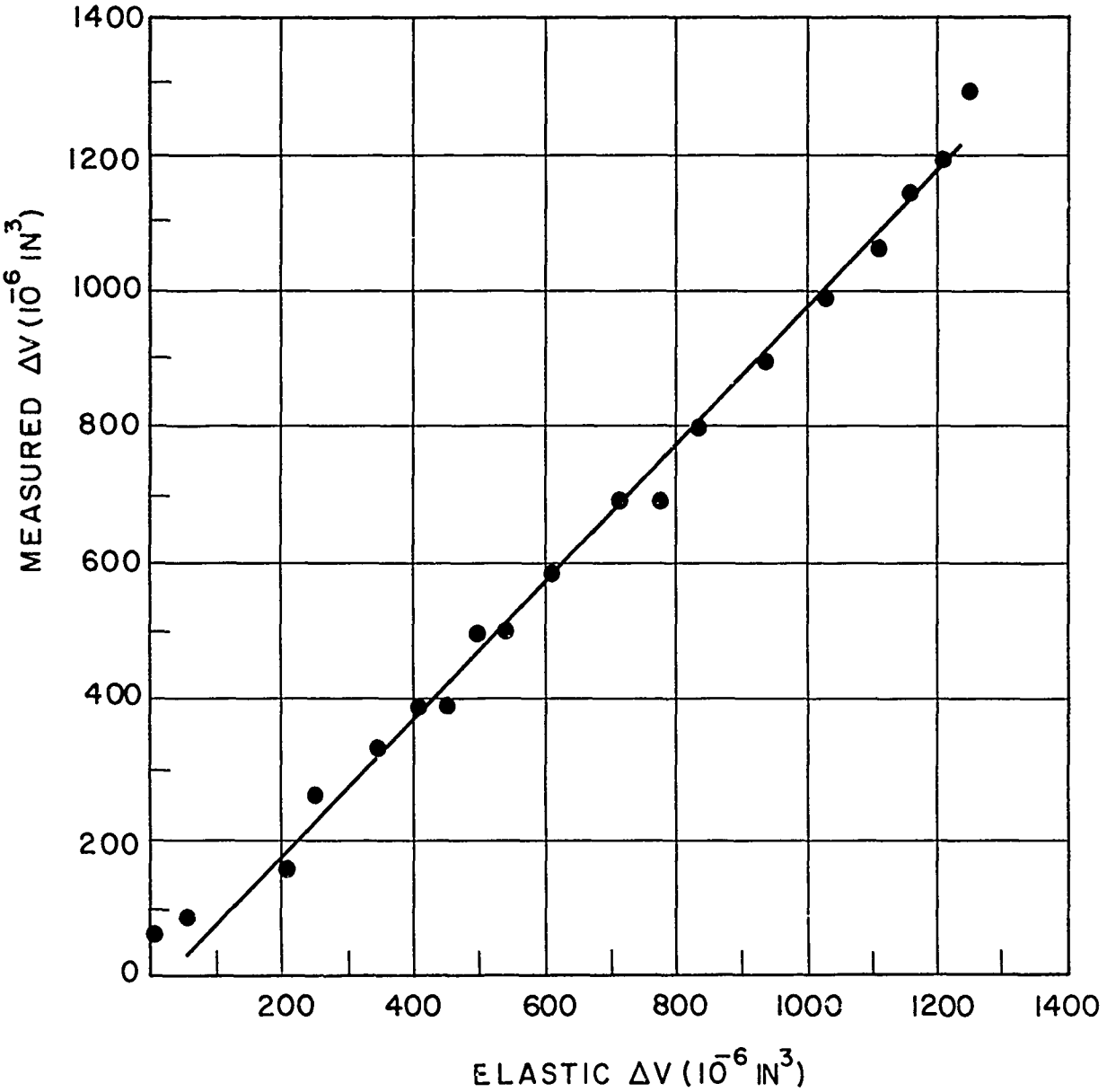

Figure 10. Volume Change in Internal Cavity of Tube.

where:

$r = 0.344$ in.
$\ell = 3.3$ in.
$\nu = 0.25$
$E = 11.4 \times 10^6$ psi.

Figure 10 indicates that the measured volume change is almost entirely elastic thus lending further support to the absence of anisotropy in Zamak-3 tubes.

INITIAL YIELDING

The yield stress is defined here as the proportional limit stress since for all practical purposes the proportional limit stress is also the elastic limit stress. This point was checked during one test run by a program of loading and unloading, each subsequent loading stopping at a higher stress. The plastic strains at zero stress showed the stress at unloading for which plastic deformation began. In this case the proportional limit stress appeared to coincide with the elastic limit stress.

For combined load tests, the measured σ_z and σ_θ were plotted against the largest measured strain. Stress values were noted at which the plot deviated from linearity. The pair of stress values used were in all cases a pair of values that had been observed at a given time. Of course, determination of the exact proportional limit is a difficult task and might be expected to appreciable scatter in results. Another alternative would be to use an offset yield strength but a consistent measure of this would require plotting of some type of effective stress-effective strain curve. The latter technique was considered to be too indirect since in effect it requires an assumption to be made for the yield criterion.

In all of the tests reported here, measurements of strain were made in axial, circumferential, and 45° directions along with measurements of axial force and internal pressure or torque. It was possible in nearly every case to measure strains up to the point of fracture.

Figure 11 is a plot in the octahedral plane of initial data for 78°F. The x-y coordinate system shown can be used to locate points in the octahedral plane. These x-y coordinates are related to the principal stresses σ_1 and σ_2 ($\sigma_3 = \sigma_r = 0$) as follows:

$$x = 1/\sqrt{2}\,(-\sigma_1 + \sigma_2)$$

$$y = -\,1/\sqrt{6}\,(\sigma_1 + \sigma_2). \qquad (53)$$

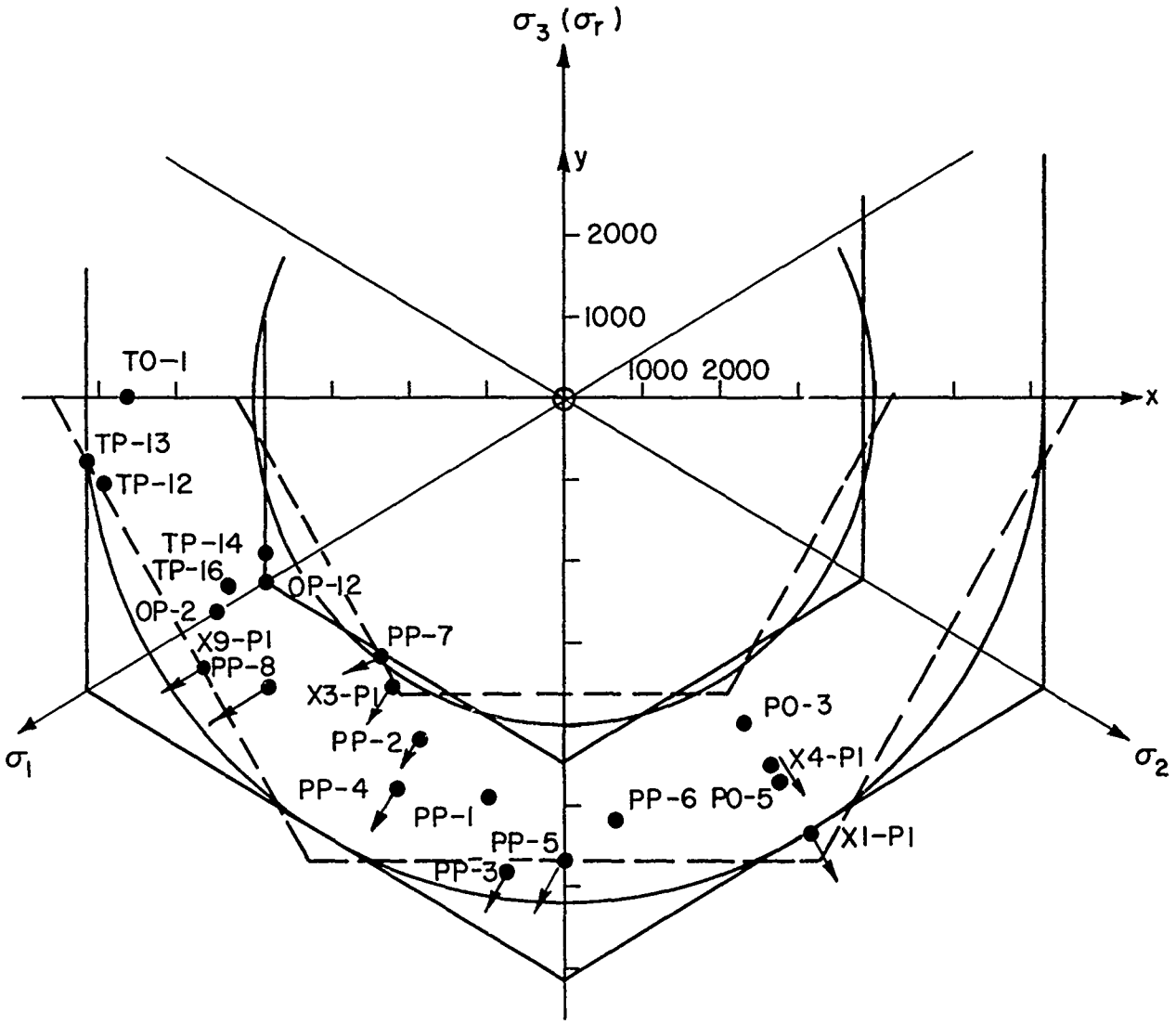

Figure 11. Initial Yield Data at 78°F.

The various numbers identify the data point with the test number. Those bearing the letters PP or X are from runs in combined tension and internal pressure, those bearing the letters OP are from pure tension runs, those bearing the letters TP are from combined tension and torsion tests, those marked PO are from pure internal pressure runs, and those bearing the letters TO are from pure torsion tests. Points X1-P1 and X4-P1 are from a test run in which internal pressure only was applied.

The circles shown would be a pair of yield surfaces containing all data points assuming the Mises criterion applies. For the inner circle $\sigma_0 = 4950$ psi, where σ_0 is the tensile yield stress, and for the outer circle $\sigma_0 = 7550$ psi. The Tresca yield criterion plots as a hexagon on the octahedral plane and the bounding hexagons for the data are shown in solid lines. For the inner solid hexagon $\sigma_0 = 5450$ psi and for the outer solid hexagon $\sigma_0 = 8700$ psi. Finally the dashed hexagons correspond to the maximum reduced stress criterion and again bounding figures are shown. For the inner dashed hexagon $\sigma_0 = 4450$ psi and for the outer dashed hexagon $\sigma_0 = 6970$ psi. The degree of scatter in the data obviate the selection of a particular yield criterion. However, the yield surfaces having plane sides appear to fit the data as well as the Mises criterion and will be used in the later analysis of strain hardening. Further an isotropic yield criterion appears to be valid.

Figure 12 is a plot in the octahedral plane of initial yield data for 32°F. All of the test symbols have been defined above. The circles in Figure 12 represent the bounding values of the Mises criterion, the inner circle corresponding to $\sigma_0 = 5030$ psi and the outer circle to $\sigma_0 = 7060$ psi. The solid hexagons represent the Tresca criterion. For the inner solid hexagon, $\sigma_0 = 5230$ psi and for the outer solid hexagon, $\sigma_0 = 8050$ psi. The maximum reduced stress criterion is represented by the dashed hexagons with the inner dashed hexagon corresponding to $\sigma_0 = 4380$ psi and the outer to $\sigma_0 = 6920$ psi. Note that the yield values for the two testing temperatures are nearly the same.

These yield surfaces are drawn, however, without considering points PP-11 and PP-12. Both of these points lie well outside the yield surfaces that bound the other points. This could be interpreted as the appearance of anisotropy but data discussed earlier indicate the material is isotropic. At present it is suggested that these stress combinations, which represent the largest value of mean stress at the lower test temperature, do imply an effect of mean stress on the yielding process. However the nature of the effect is rather difficult to explain.

It is also to be noted that Figure 12 shows data for both tension and compression (negative σ_1-axis) tests and that the yield in tension and compression appear to be equal. This constitutes some evidence that there is no effect of mean stress on yielding in this material.

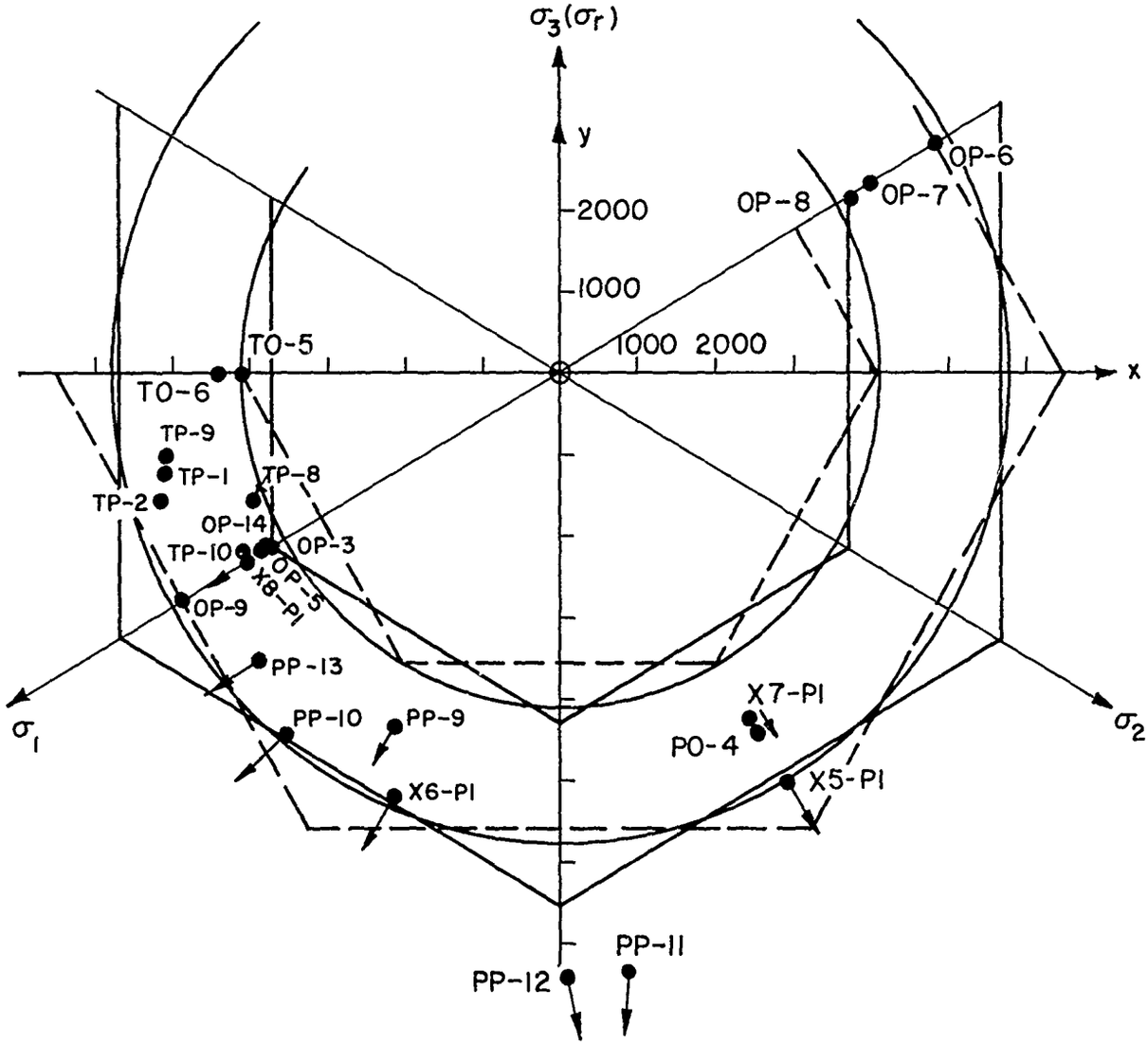

Figure 12. Initial Yield Data at 32°F.

STRAIN HARDENING

A series of multiple loading path tests were performed to afford a check of the various strain hardening theories. The general procedure in these tests was to load first along a given path (radial in all cases) to a point well beyond the initial yield surface, then to completely unload the specimen and to reload again along a second radial loading path to fracture. All of the data were obtained using combinations of tension and internal pressure so that rotation of the principal axis of stress would not occur during the loading program.

In all of the analysis presented, the Tresca yield criterion and the maximum reduced stress criterion of yielding are used because of their relative simplicity in connection with the kinematic hardening hypothesis.

Figure 13 gives the results for test X1 which was performed at 78°F. Initial loading in this case was internal pressure alone. The point designated X1-P1 represents initial yielding while X1-P1 max denotes the largest stress combination reached for the first path. Hexagon ABCDEFA represents the initial Tresca yield surface and hexagon GHIJKLG represents the initial maximum reduced stress yield surface. These are outlined in dashed lines. Note that X1-P1 max lies on a subsequent yield surface denoted by the solid hexagons A'B'C'D'E'F'A' and G'H'I'J'K'L'G'. The second loading was a combination of tension and internal pressure and point X1-P2 is the yield point during this second loading.

It is apparent that yielding on secondary loading did occur at approximately the point predicted by the kinematic hardening theory. Isotropic hardening would predict a yield stress-combination that is much too large in comparison with the observed yield data on second loading.

Figures 14, 15, and 16 present other multiple loading path results for 78°F. Figures 17, 18, 19, and 20 are similar results obtained at 32°F. Designation of points on these figures in analogous to that described above. In Figure 15, the data for yielding on second load indicate that the translated maximum reduced stress criterion predicts a yield stress-combination which is much too small. The other test data indicate that the kinematic hardening theory in conjunction with either Tresca or maximum reduced stress yield criteria give good predictions for the stress combination to produce yielding on second loading. This is true even for fairly large translations of the yield surface.

Actually the data presented here are insufficient to firmly establish that the yield surface translates as a rigid body. Thus it is possible that deformation of the yield surface might occur or that the correct strain hardening theory is the piecewise linear one proposed by Hodge. Additional test data would be required to resolve this point.

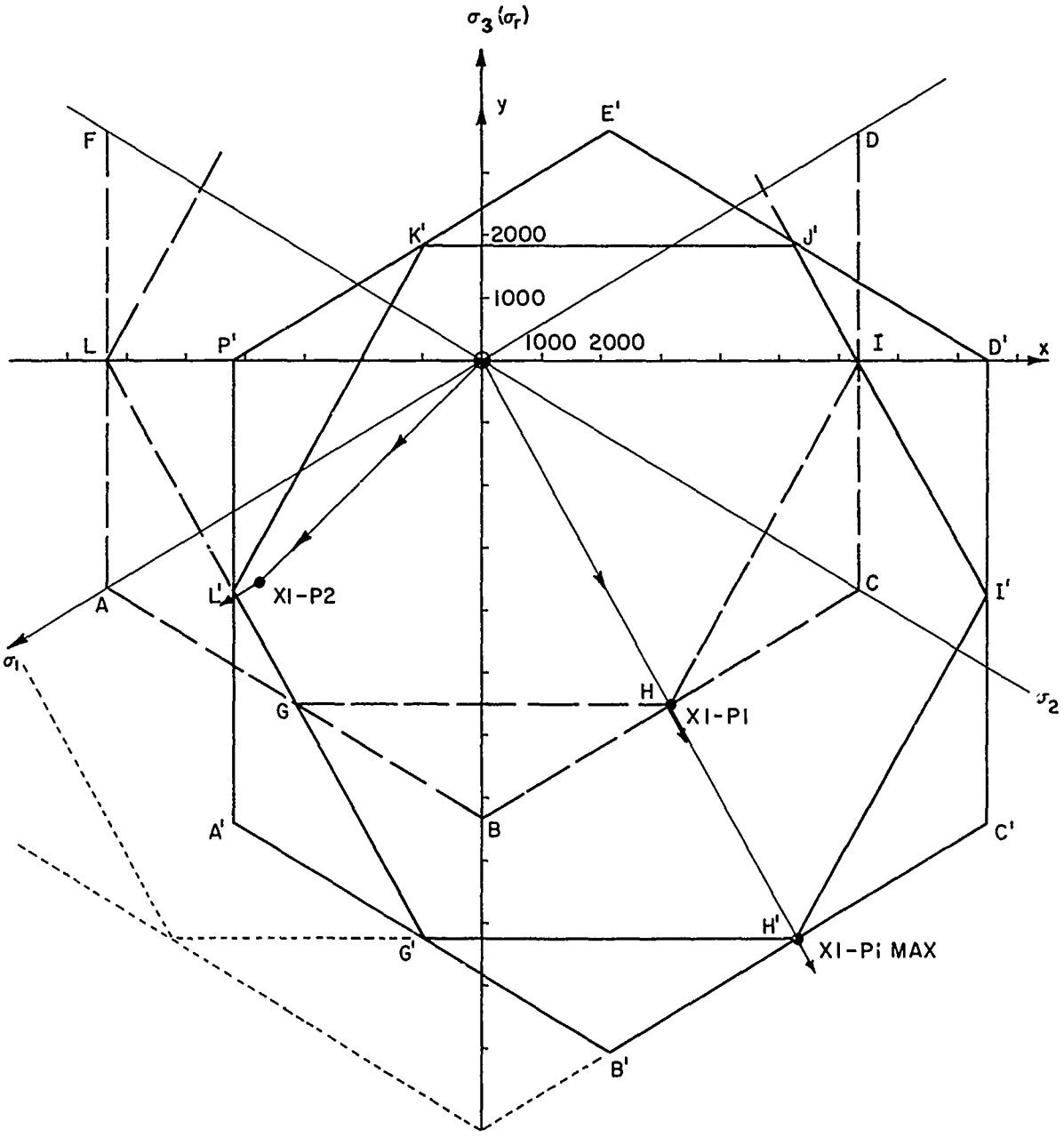

Figure 13. Strain-Hardening Behavior, Test X-1. 78°F.

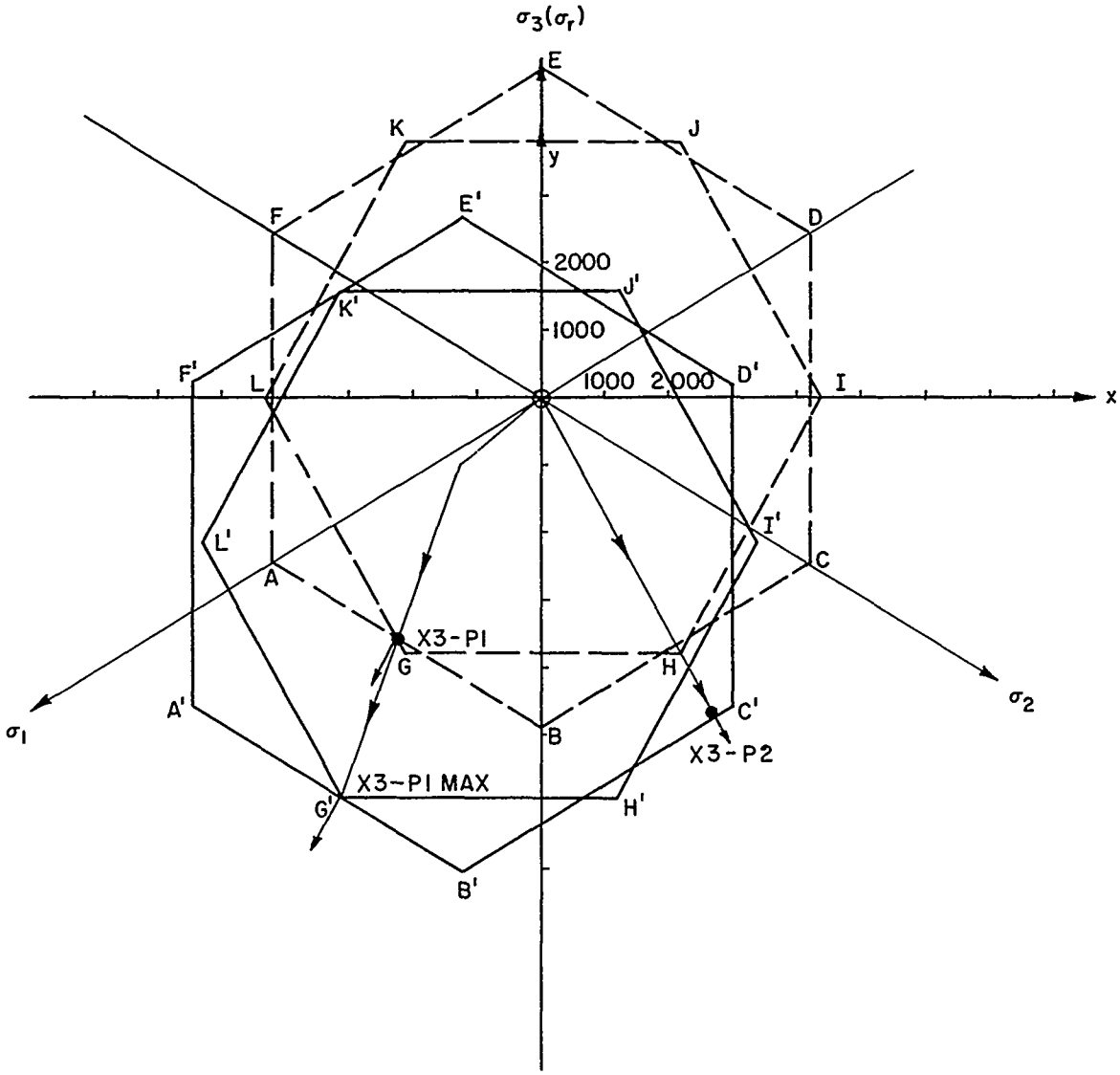

Figure 14. Strain-Hardening Behavior, Test X-3. 78°F.

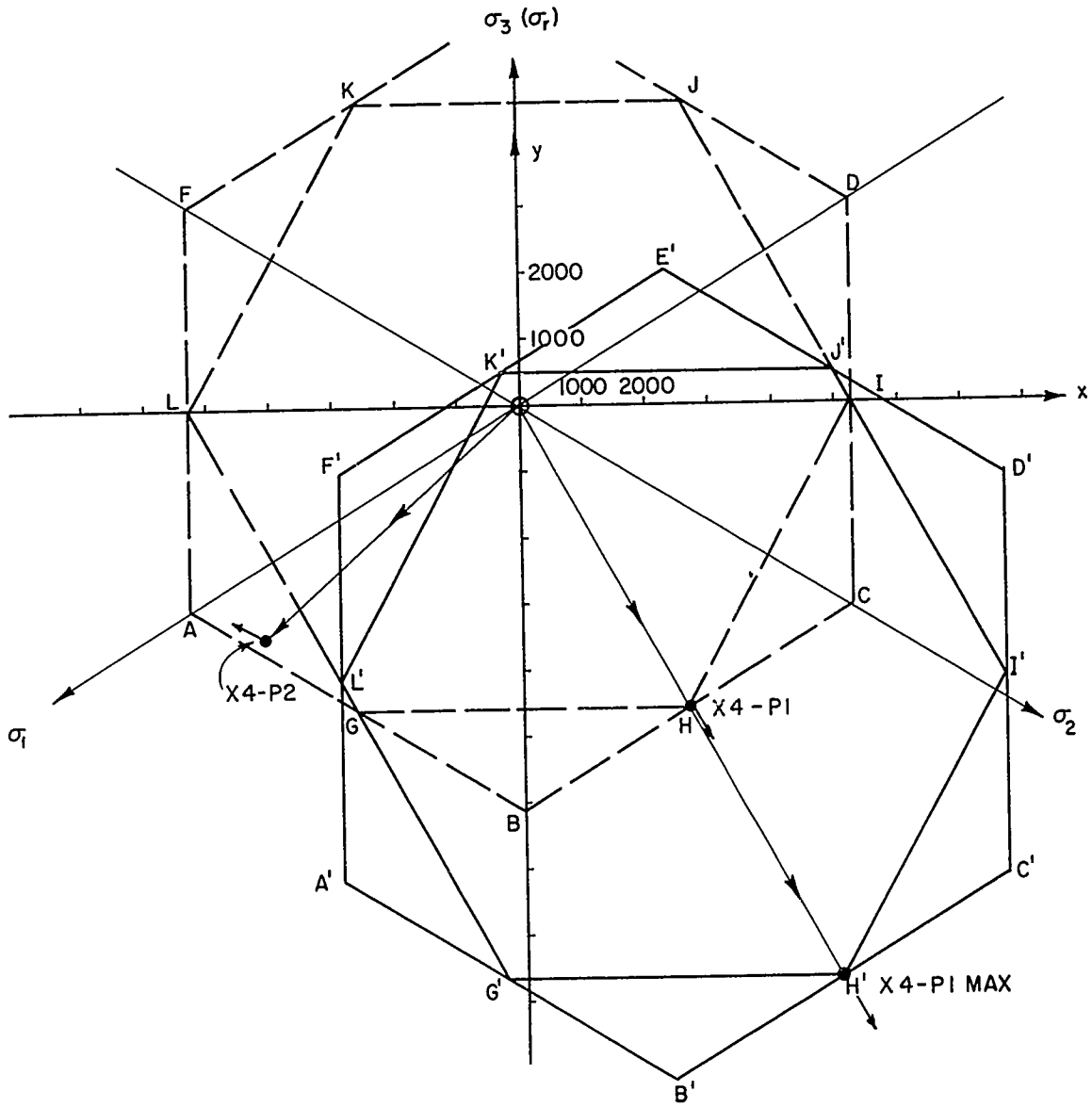

Figure 15. Strain-Hardening Behavior, Test X-4. 78°F.

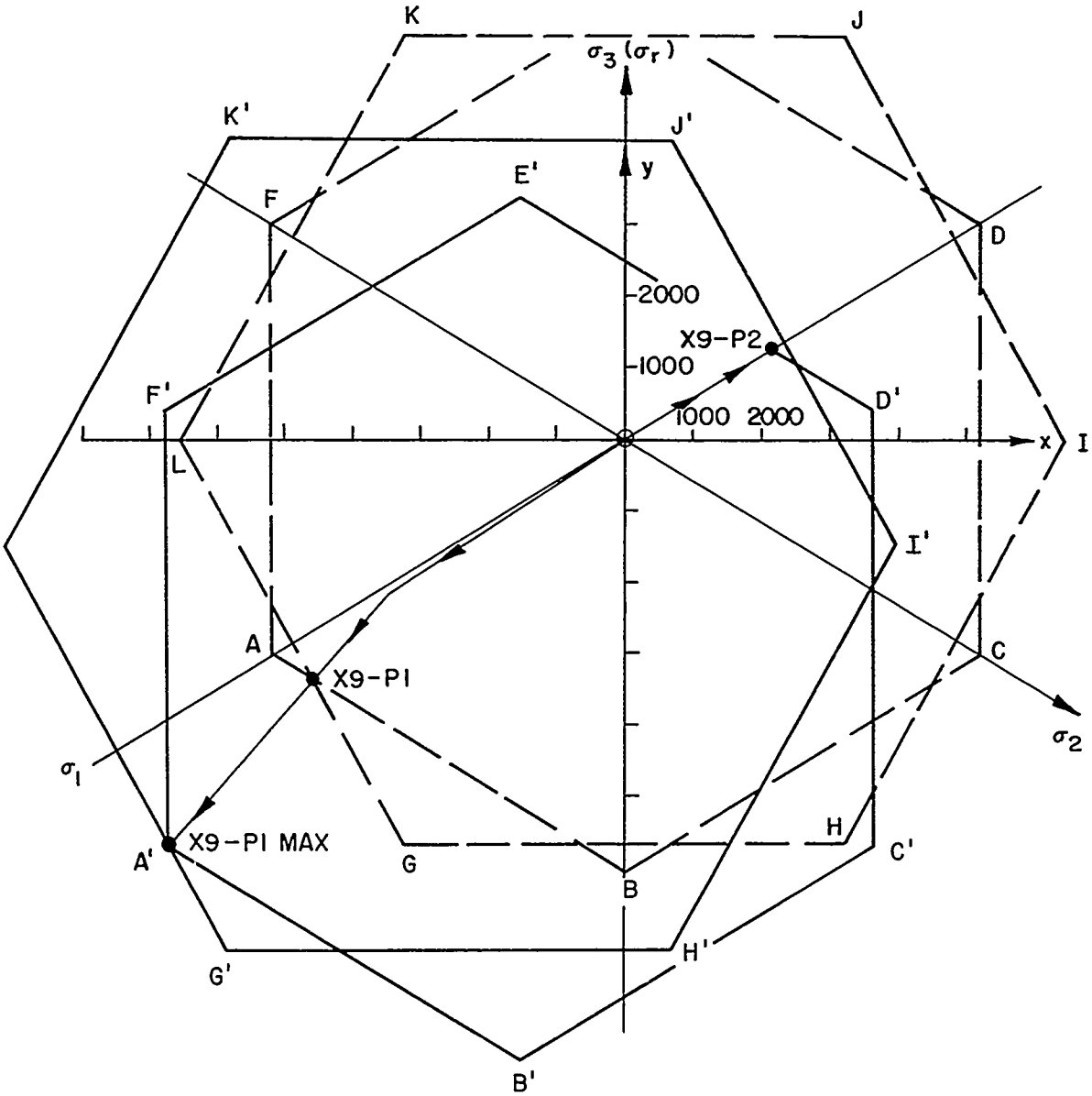

Figure 16. Strain-Hardening Behavior, Test X-9. 78°F.

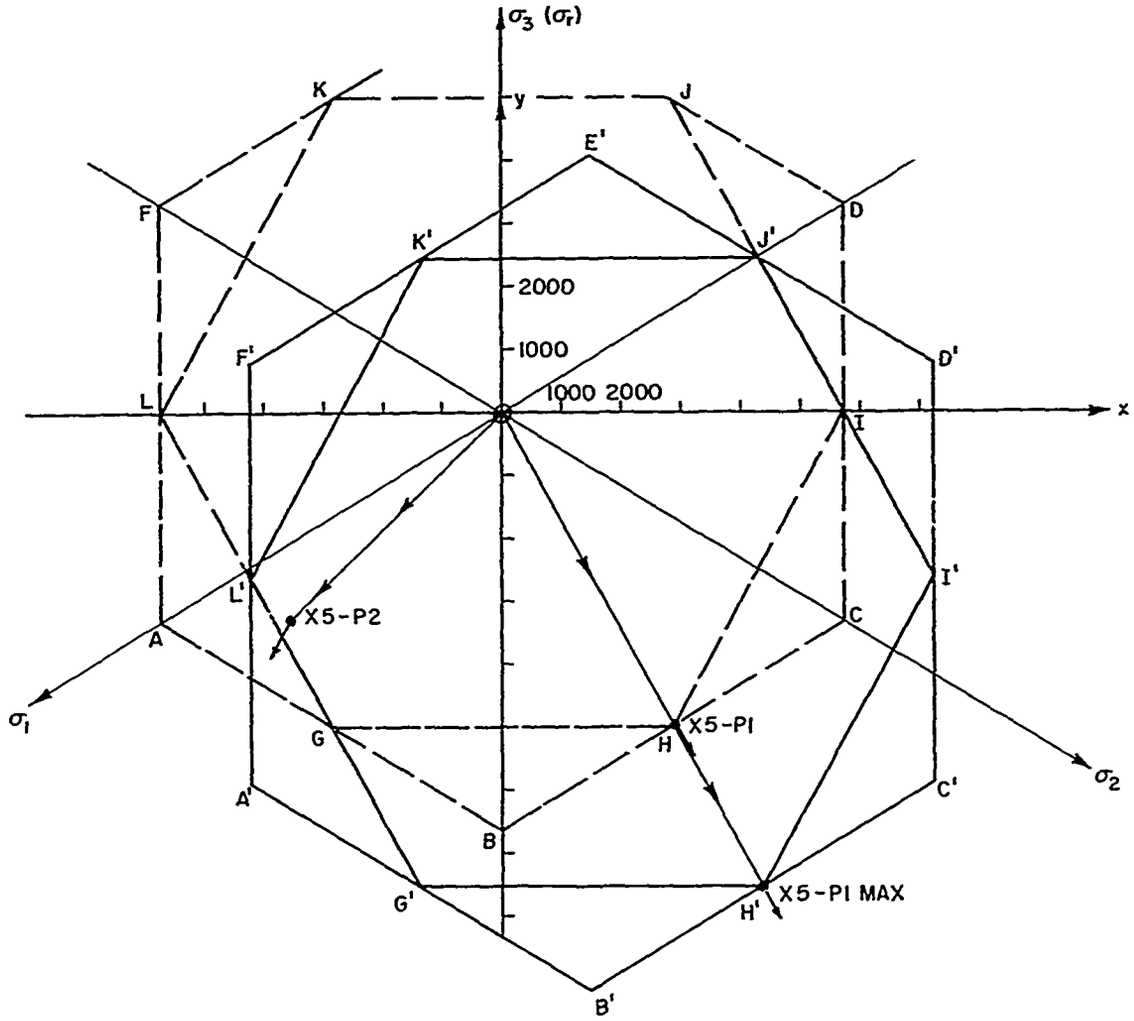

Figure 17. Strain-Hardening Behavior, Test X-5. 32°F.

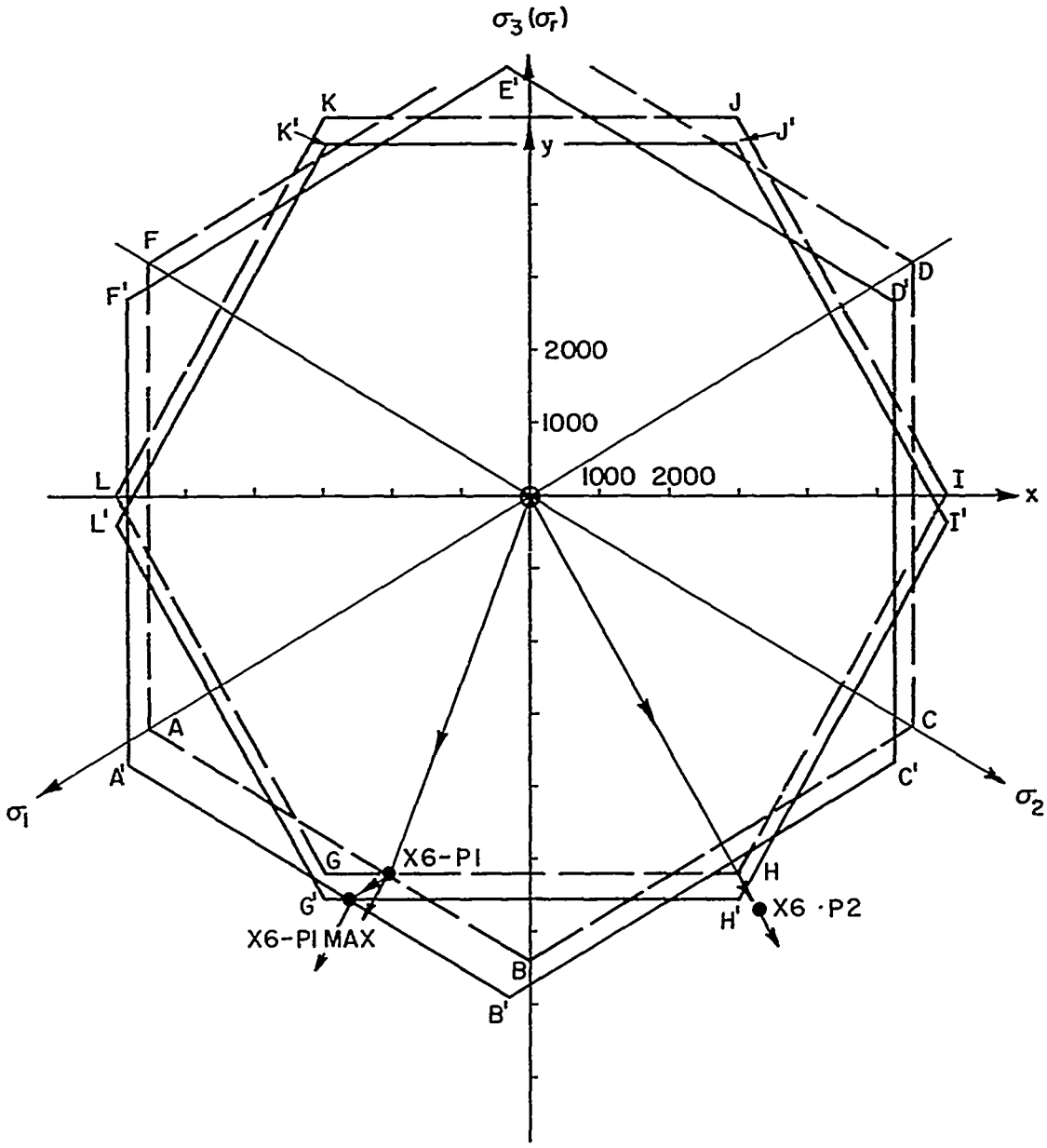

Figure 18. Strain-Hardening Behavior, Test X-6. 32°F.

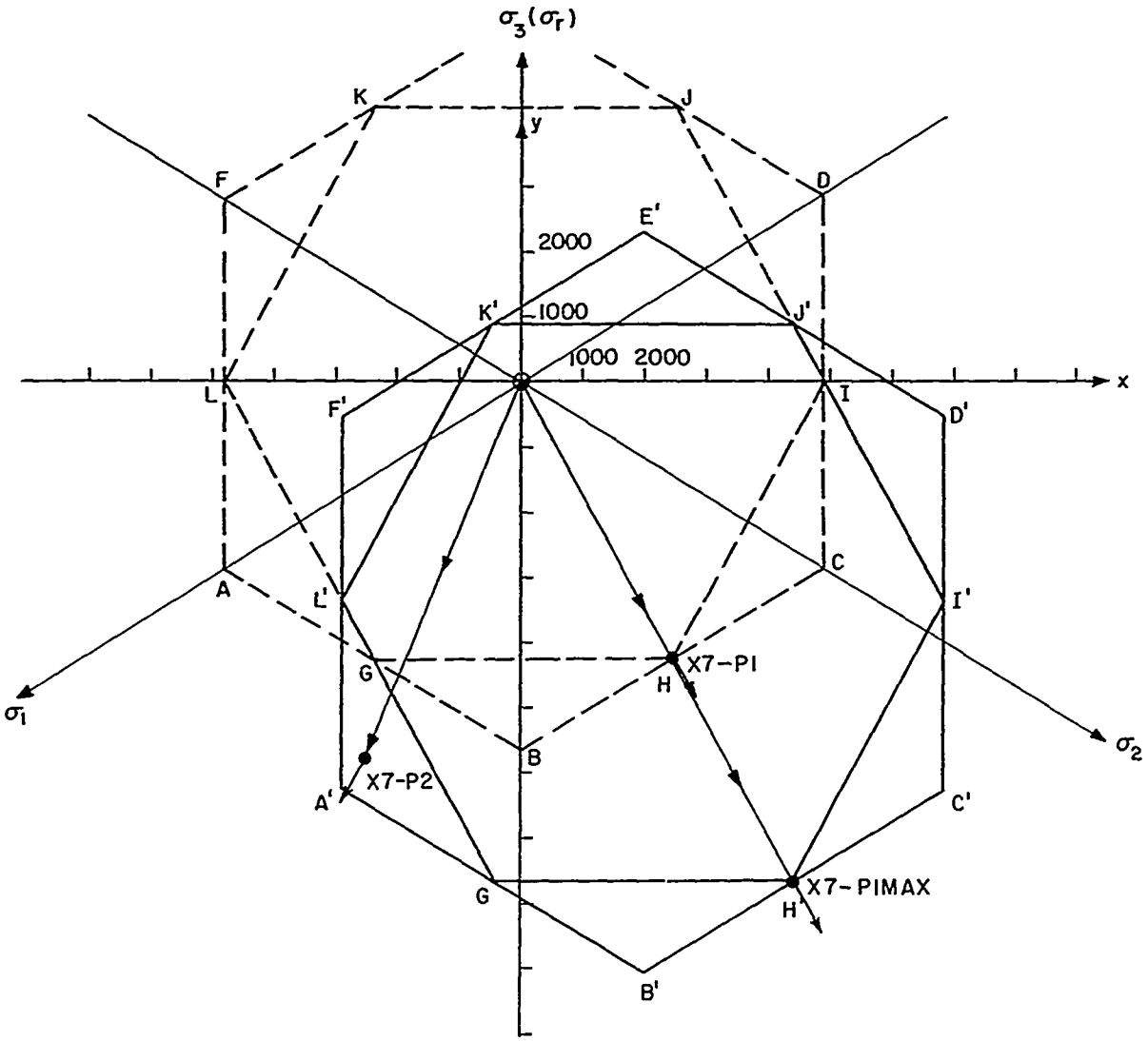

Figure 19. Strain-Hardening Behavior, Test X-7. 32°F.

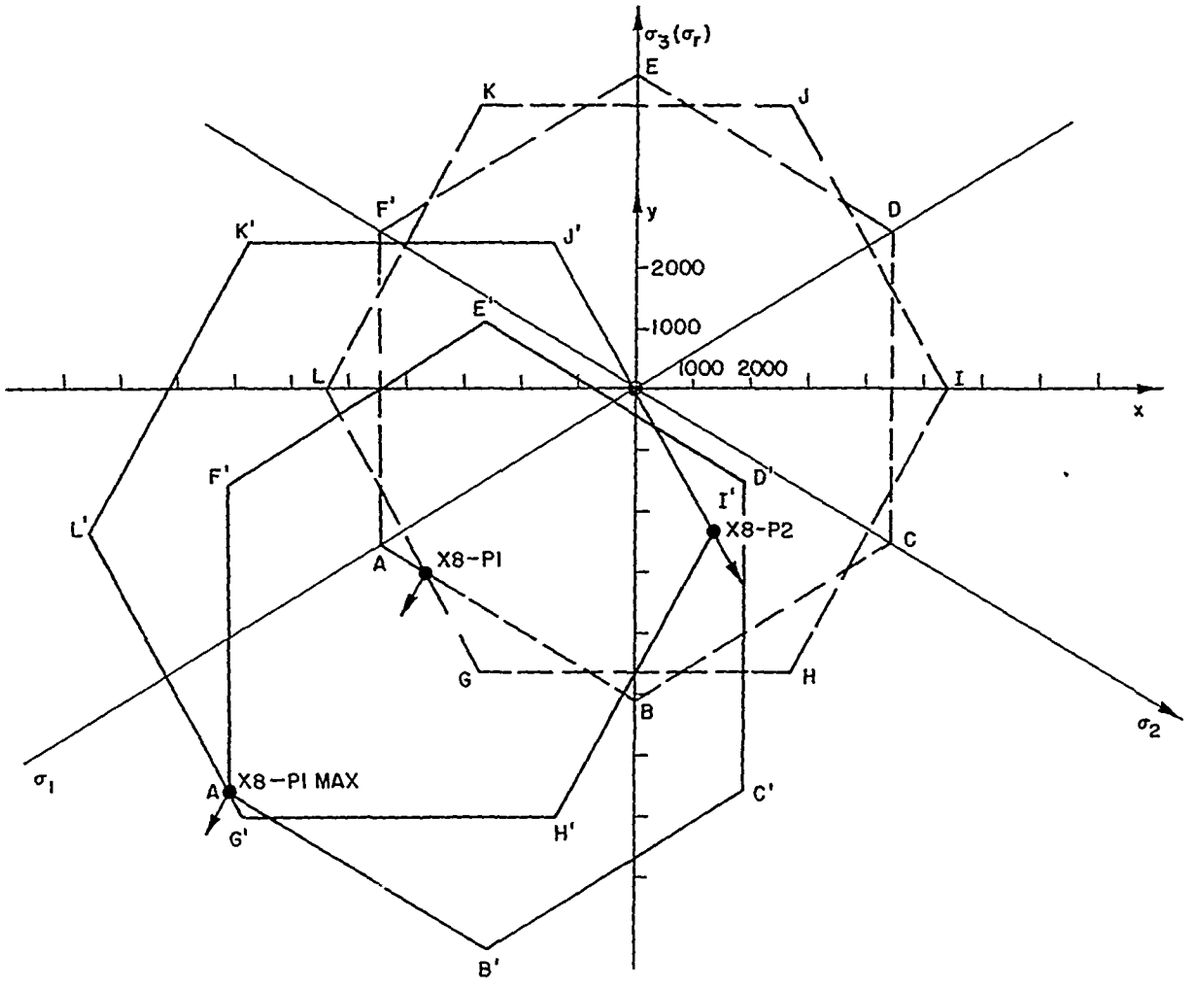

Figure 20. Strain-Hardening Behavior, Test X-8. 32°F.

FRACTURE

Observed stresses at fracture for combined tension and internal pressure are plotted in Figure 21. Circles represent data at 78°F and crosses represent data at 32°F.

These data are presented on a graph of σ_θ versus σ_z, the principal stresses, since there is no reason to expect that fracture is independent of mean stress and the octahedral plane is useless. All data points roughly follow the maximum normal stress criterion of rupture, with a stress at rupture of about 27,000 psi being appropriate. All of these data points represent "brittle" behavior, the principal strain at fracture falling in the range 0.004 to 0.007. The only "ductile" behavior at either test temperature was in pure torsion. Here the principal strains reached 0.020 before the test was terminated because of insufficient twisting capacity.

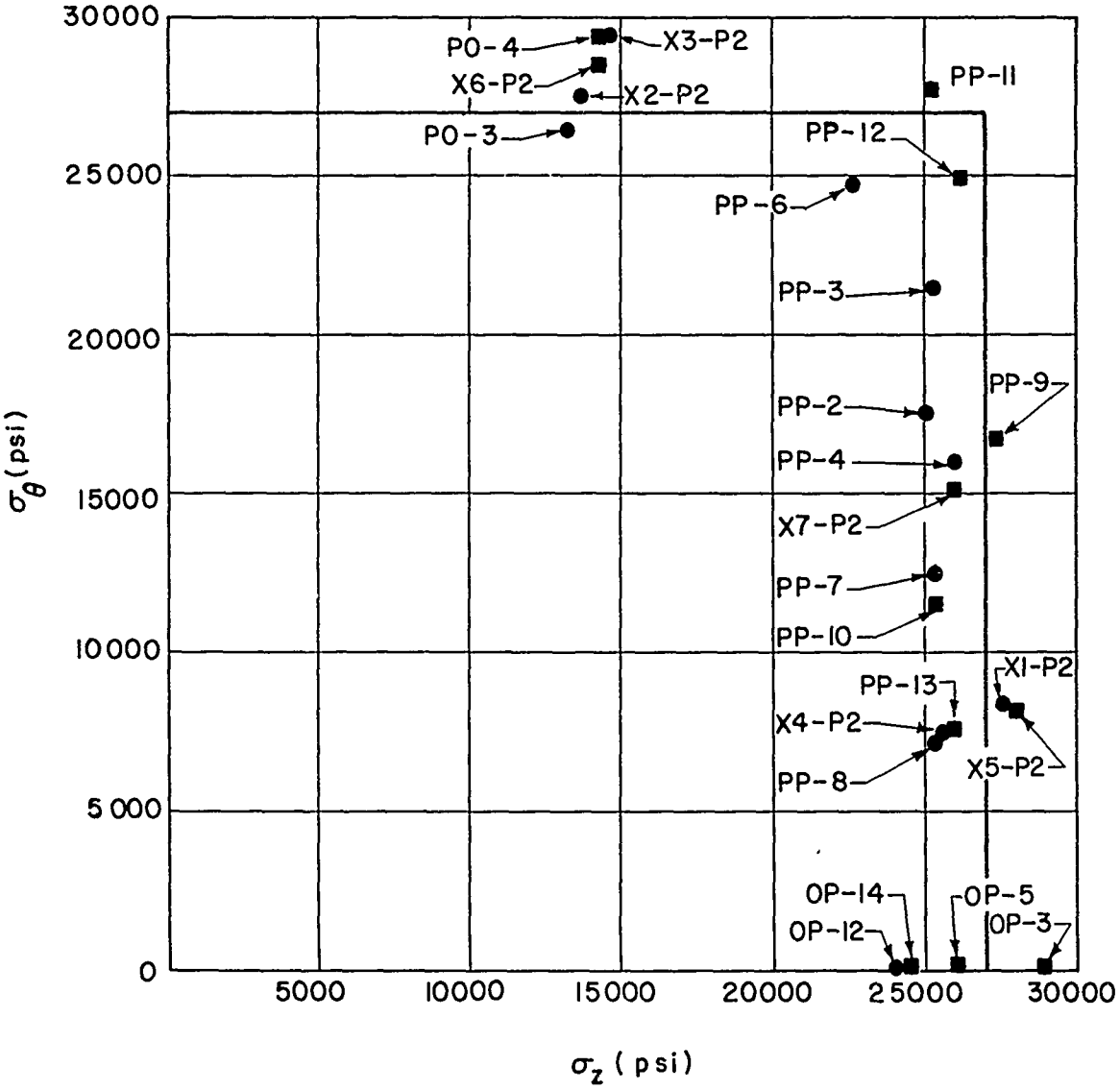

Figure 21. Fracture Data for Combined Tension and Internal Pressure.

CONCLUSIONS

The experimental data presented in the previous section appear to justify the following conclusions:

1. The Zamak-3 tubes are isotropic or at most exhibit anisotropy which is rotationally symmetric about the axis of a specimen. The latter seems unlikely.

2. Although there is scatter in the test results, it appears that initial yield criteria which assume isotropy and independence of mean stress are applicable. Certain unexplained anomalies appear at high mean stresses however.

3. The initial yield stress is in the same range for tests at 32°F and 78°F.

4. Strain-hardening behavior can be predicted by a kinematic or piecewise linear theory in conjunction with the Tresca yield criterion.

5. Fracture under brittle conditions is satisfactorily prediced by a maximum normal stress theory of fracture.

It should be noted that further analysis of these data will be presented in a special report constituting the Ph.D. thesis of one of the investigators (D. R. Jenkins). This special report will be available in early summer.

REFERENCES

1. Clark, S. K., Gascoigne, H. E., Jenkins, D. E., and Wolf, L. W., Effect of State of Stress on the Failure of Metals at Various Temperatures, WADD TR 60-234, The University of Michigan, March, 1960 Contract No. AF 33(616)-6041 .

2. Clark, S. K., Haythornthwaite, R. M., and Jenkins, D. R., Effect of State of Stress on the Failure of Metals at Various Temperatures, WADD TR 60-869, The University of Michigan, January, 1961 Contract No. AF 33(616)-6041 .

3. Griffith, A. A., "The Theory of Rupture," Proceedings of the First International Congress for Applied Mechanics (Delft), 1924, pp. 55-63.

4. Drucker, D. C., "A More Fundamental Approach to Plastic Stress-Strain Relations," Proceedings of the First U. S. National Congress of Applied Mechanics, 1951, ASME (1952), pp, 487-491.

5. von Mises, R., "Mechanik der plastischen Formanderung von Kristallen," Keitschrift für Angew Math und Mech, vol. 8, 1928, pp. 161-185.

6. Haythornthwaite, R. M., "Range of Yield Condition in Ideal Plasticity," Journal of the Engineering Mechanics Division, Proceedings of the American Society of Civil Engineers, vol. 87, No. EM6, December, 1961

7. Hill, R., The Mathematical Theory of Plasticity, Oxford University Press, 1950, pp. 23-49.

8. Prager, W., "The Theory of Plasticity: A Survey of Recent Achievements," Proceedings of the Institution of Mechanical Engineers, vol. 169, 1955, pp. 41-57.

9. Shield, R. T., and Zeigler, H., "On Prager's Hardening Rule," Zeitschrift für Angewandte Mathematik und Physik, vol. 9a, 1958, pp. 260-276.

10. Hodge, P. G., Jr., "A General Theory of Piecewise Linear Plasticity Based on Maximum Shear," Journal of the Mechanics and Physics of Solids, vol. 5, 1957, pp. 242-260.

11. Sanders, J. L., Jr., "Plastic Stress-Strain Relations Based on Linear Loading Functions," Proceedings of the Second U. S. National Congress of Applied Mechanics, 1954, ASME (1955), pp. 455-460.

12. Hill, R., loc. cit., p. 318.

13. Taylor, G. I., and Quinney, H., "Plastic Distortion of Metals," Philosophical Transactions of the Royal Society, London, A, vol. 230, 1931, p. 323.

14. Pugh, H.L.D., "A Note on a Test of the Plastic Isotropy of Metals," Journal of Mechanics and Physics of Solids, vol. 1, 1953, pp. 284-286.

Aeronautical Systems Division, Wright-Patterson AF Base, Ohio.
Rpt No. WADD-TR-60-869, Part II. EFFECT OF STATE OF STRESS ON THE FAILURE OF METALS AT VARIOUS TEMPERATURES. Final report, June 62, 42p. incl illus., 14 refs.
Unclassified Report

Experimental observations of initial yielding, strain hardening, and fracture of Zamak-3 tubes for various states of combined stress are presented. Testing temperatures of 32°F and 78°F were employed. These observations are compared with predictions of Mises, Tresca, and maximum reduced stress theories of initial

(over)

UNCLASSIFIED

1. Stresses
2. Failure
3. Zinc-alloy
I. AFSC Project 7353 Task 735301
II. Contract AF 33 (616)-6041
III. Univ. of Michigan Ann Arbor, Mich
IV. R. M. Haythornthwaite, D. R. Jenkins
V. Aval fr OTS
VI. In ASTIA collection

UNCLASSIFIED

Aeronautical Systems Division, Wright-Patterson AF Base, Ohio.
Rpt No. WADD-TR-60-869, Part II. EFFECT OF STATE OF STRESS ON THE FAILURE OF METALS AT VARIOUS TEMPERATURES. Final report, June 62, 42p. incl illus., 14 refs.
Unclassified Report

Experimental observations of initial yielding, strain hardening, and fracture of Zamak-3 tubes for various states of combined stress are presented. Testing temperatures of 32°F and 78°F were employed. These observations are compared with predictions of Mises, Tresca, and maximum reduced stress theories of initial

(over)

UNCLASSIFIED

1. Stresses
2. Failure
3. Zinc-alloy
I. AFSC Project 7353 Task 735301
II. Contract AF 33 (616)-6041
III. Univ. of Michigan Ann Arbor, Mich
IV. R. M. Haythornthwaite, D. R. Jenkins
V. Aval fr OTS
VI. In ASTIA collection

UNCLASSIFIED

yielding and with isotropic and kinematic theories of strain hardening. Fracture data are compared with the Griffith theory of rupture for brittle materials. It is concluded that Zamak-3 behaves as an essentially isotropic material in which yielding is independent of mean stress. Multiple loading path test results agree rather well with the predictions of kinematic hardening theory in conjunction with the Tresca yield criterion. Fracture results conform to a maximum normal stress theory which coincides with the Griffith theory for the stress combinations investigated.

UNCLASSIFIED

UNCLASSIFIED

yielding and with isotropic and kinematic theories of strain hardening. Fracture data are compared with the Griffith theory of rupture for brittle materials. It is concluded that Zamak-3 behaves as an essentially isotropic material in which yielding is independent of mean stress. Multiple loading path test results agree rather well with the predictions of kinematic hardening theory in conjunction with the Tresca yield criterion. Fracture results conform to a maximum normal stress theory which coincides with the Griffith theory for the stress combinations investigated.

UNCLASSIFIED

UNCLASSIFIED

Aeronautical Systems Division, Wright-Patterson AF Base, Ohio.
Rpt No. WADD-TR-60-869, Part II. EFFECT OF STATE OF STRESS ON THE FAILURE OF METALS AT VARIOUS TEMPERATURES. Final report, June 62, 42p. incl illus., 14 refs.
Unclassified Report

Experimental observations of initial yielding, strain hardening, and fracture of Zamak-3 tubes for various states of combined stress are presented. Testing temperatures of 32°F and 78°F were employed. These observations are compared with predictions of Mises, Tresca, and maximum reduced stress theories of initial

(over)

UNCLASSIFIED

1. Stresses
2. Failure
3. Zinc-alloy
I. AFSC Project 7353 Task 735301
II. Contract AF 33 (616)-6041
III. Univ. of Michigan Ann Arbor, Mich
IV. R. M. Haythornthwaite, D. R. Jenkins
V. Aval fr OTS
VI. In ASTIA collection

UNCLASSIFIED

yielding and with isotropic and kinematic theories of strain hardening. Fracture data are compared with the Griffith theory of rupture for brittle materials. It is concluded that Zamak-3 behaves as an essentially isotropic material in which yielding is independent of mean stress. Multiple loading path test results agree rather well with the predictions of kinematic hardening theory in conjunction with the Tresca yield criterion. Fracture results conform to a maximum normal stress theory which coincides with the Griffith theory for the stress combinations investigated.

UNCLASSIFIED

UNCLASSIFIED

Aeronautical Systems Division, Wright-Patterson AF Base, Ohio.
Rpt No. WADD-TR-60-869, Part II. EFFECT OF STATE OF STRESS ON THE FAILURE OF METALS AT VARIOUS TEMPERATURES. Final report, June 62, 42p. incl illus., 14 refs.
Unclassified Report

Experimental observations of initial yielding, strain hardening, and fracture of Zamak-3 tubes for various states of combined stress are presented. Testing temperatures of 32°F and 78°F were employed. These observations are compared with predictions of Mises, Tresca, and maximum reduced stress theories of initial

(over)

UNCLASSIFIED

1. Stresses
2. Failure
3. Zinc-alloy
I. AFSC Project 7353 Task 735301
II. Contract AF 33 (616)-6041
III. Univ. of Michigan Ann Arbor, Mich
IV. R. M. Haythornthwaite, D. R. Jenkins
V. Aval fr OTS
VI. In ASTIA collection

UNCLASSIFIED

yielding and with isotropic and kinematic theories of strain hardening. Fracture data are compared with the Griffith theory of rupture for brittle materials. It is concluded that Zamak-3 behaves as an essentially isotropic material in which yielding is independent of mean stress. Multiple loading path test results agree rather well with the predictions of kinematic hardening theory in conjunction with the Tresca yield criterion. Fracture results conform to a maximum normal stress theory which coincides with the Griffith theory for the stress combinations investigated.

UNCLASSIFIED

UNCLASSIFIED